

1 **Review comments are in black, while responses to the reviewer are in red. When text**
2 **from the manuscript is quoted, new text is in bold face. The authors would like thank**
3 **both reviewers for both their positive feedback, as well as their constructive criticism,**
4 **which improved the manuscript. We revise the text as suggested by the reviewers.**

5

6 **Anonymous Referee #1:**

7

8 **1 General comments**

9 The modelling study by Zhang et al. that is presented here attempts to assess the effect of the
10 spatial variability in the elemental composition of dust sources on the transport and deposition
11 of trace elements by dust. Presently, the deposition of trace elements is often calculated from
12 bulk dust deposition, assuming a fixed elemental composition of dust; given that dust sources
13 can differ quite dramatically in their elemental composition this is a significant progress and
14 certainly justifies publication in Biogeosciences.

15 The first step in the study by Zhang et al. is the compilation of a map of soil elemental
16 composition using a high resolution soil data set from the FAO, then estimating the fractions
17 of different minerals in the different soils, following Claquin et al. (1999) and Nickovic et al
18 (2012), finally combining them with data sets on the elemental composition of different
19 minerals from the literature. As the authors acknowledge, the assumptions on the mineral
20 composition of soil types likely underestimates the variability present. The authors also note
21 that impurities in gypsum, calcite and quartz can lead to variability in trace elements that is
22 disregarded here. Very likely thus the spatial variability in dust source elemental composition
23 is underestimated by the approach taken here; nevertheless, the first-order-trends are likely
24 correct. For iron, similar attempts have been undertaken by Nickovic et al. (2013) (side-note:
25 Only the precursor to that paper, Nickovic et al., 2012, is cited) and Journet et al. (2014), but
26 the extension to more elements is a significant step that also allows a better validation.

27 The second step is then to calculate the the emission, transport and deposition of this dust,
28 using the Community Earth System Model that has already been widely used for dust
29 transport modelling before. The novel aspect here is that the model now transports the
30 different elements individually, so that at each point in space and time the elemental
31 composition varies.

32 Finally, in a third step the modeled elemental composition of dust and of dust deposition are
33 verified by comparing them to a dataset of ground-based observation at a number of sites
34 around the world.

35 Although the results of the validation are somewhat mixed, the paper presents a significant
36 step forward, and I think the paper should be published after suitable revision.

37 However, before coming to my points of criticism, I'd like to mention that the whole paper is
38 still written in an English that contains too many errors to list all of them at the end of this
39 review, so I will limit myself to listing only a subset. In this form the paper cannot be
40 published and I would urge the native English speaking coauthors to help the first author to
41 rewrite it.

42 **We thank the reviewer for their comments, and have worked to ensure that the English is**
43 **improved in the resubmitted version.**

44

45

46 **2 Main points of criticism**

47 For the review of the paper I have several main points that I would like the authors to answer:

48

49 Firstly, the transport of the different elements in the dust by the earth system model is applied
50 to each element individually; in reality, the elements are bound together in different particles
51 of variable composition. The assumption of individual elemental transport is likely to
52 introduce some smoothing, i.e. an error. The situation is similar to that in marine ecosystem
53 models with variable stoichiometry, where the variable stoichiometry of individual
54 hytoplankton cells is mixed through by the ocean models advection and diffusion. For the
55 latter case, Christian (2007) has examined the magnitude of the error introduced by that
56 assumption (and generally found it to be handle-able); maybe the authors could have a look
57 into that paper and come up with a similar argumentation?

58 **In CESM, we treat eight elements as tracers in model, like dust. As the reviewer says, by**
59 **splitting the dust into parts, we are introducing an error; usually most of this error comes from**
60 **the advection algorithm itself. Of course, there is no advection algorithm that is mass**
61 **conserving, monotonic, shape preserving and computationally efficient. There is quite a bit**
62 **of literature on this issue, and we are using a state-of-the-art advection algorithm, which**
63 **minimizes many of these issues. Because in our methodology we did not include every**
64 **element that is in dust, we cannot explicitly examine the size of this error, but from other**
65 **studies (including the one cited) we can assume it is not a large source of error for our**
66 **calculation, but rather the errors associated with the source mineralogy is probably larger.**
67 **We add in the following paragraph in the methods section:**

68 **“By splitting the dust into its different mineral elements, we may add in additional**
69 **numerical errors, because the elements are transported separately. There has been**
70 **considerable work on improving advection algorithms in atmospheric models, and here**
71 **we use the finite volume advection algorithm as part of the CAM [Lin and Rood, 1997].**
72 **While no advection scheme is perfectly mass conserving, monotonic, shape preserving**
73 **and computational efficient, this scheme does a good job of balancing these multiple**
74 **goals and maintaining strong gradients required in modeling atmospheric constituents**
75 **(e.g. [Rasch et al., 2006]). Studies focused on elemental distributions in ocean models**
76 **have suggested the relatively small uncertainties associated with these types of**
77 **numerical errors (e.g. [Christian, 2007]), and compared with the errors in the source**
78 **distribution of the minerals, errors from advection are likely to be small and are**
79 **neglected here.”**

80

81 **And we also add in a sentence in the conclusions highlighting that we think the soil map is the**
82 **largest source of uncertainty in this study.**

83

84

85 Secondly, the authors validate their model to a large extent with averaged elemental fractions
86 in dust (line 21 to 23 on page 17505), but do not describe adequately how they calculated the
87 average. Did they calculate the elemental fractions and then average those temporally for each
88 location, or did they first average the amount of element and dust (or element and dust flux) at

89 a location and then form the ratio of the two? And then, averaging the elemental fractions at
90 the different validation sites, did they weigh the fractions by the amount of dust or dust flux?
91 Depending on what you do the results may differ quite a bit. It would be interesting to see
92 method of averaging affect e.g. the elemental fraction of iron (lines 8-10 in page 17506).

93 This is an important point, and we agree that we should discuss this more. We add in the
94 following calculation into the section identified by the reviewer, and we add to each table and
95 figure caption how the % is calculated to be clear. In this study we calculate the elemental
96 fractions and average those temporally for each site. We have added the following paragraph
97 into the paper to illustrate this point better:

98 **“For this comparison (above), we calculate the elemental fractions and average**
99 **the fractions temporally for each site and compare to observations, but alternatively, we**
100 **could average the elemental concentrations and divide by the elemental dust**
101 **concentrations instead, and this will make a difference in our interpretations. For**
102 **example, taking site 2-Tazhong, the averaged fraction is 3.5% when we calculate the**
103 **fractions of iron firstly and average those temporally. However, when we calculate the**
104 **averaged iron mass and dust mass separately, their ratio is 2.3%. For site3-Yulin, the**
105 **ratio is 3.6% and 3.1% for the first method and second method, respectively. This**
106 **difference maybe due to dust storm events. For this comparison, we use the first**
107 **method, as we think it is more suitable for our goal of simulating the % of each element**
108 **correctly.”**

109
110

111 Thirdly, the authors describe that the comparison between modeled and observed elemental
112 fractions is not very good for two elements, namely magnesium and manganese (see e.g. the
113 correlations in table 3). However, the authors do not discuss why that is. I suspect that it has
114 to do with the uncertainty in the assumed average mineral composition (table 1); calcite e.g.
115 often contains quite a bit of magnesium, but the assumed fraction in table 1 is zero. Maybe the
116 authors could try to discuss the propagation of errors in table 1 onto their results a bit.

117 This is a very good question to answer. Originally we just discussed in paper separately with
118 Table1 using **“Underestimation of Mg and Mn could be due to a deficiency of minerals**
119 **contaning high concentrations of Mg and Mn in our model, as dolomite(MgCO₃) or**
120 **palygorskyte ((Mg,Al)₂Si₄O₁₀(OH)·4(H₂O)) are often identified in dust particles for**
121 **Mg. Moreover, it is known that the chemical composition of minerals could be variable**
122 **according to the regional origin of minerals and possible impurities. For example, the**
123 **Mg content in calcite ranges from 0% to 2.7% in the natural environment.”** Now we
124 have added in P17507 with the sentence of **“But in this study, the assumed fraction of Mg**
125 **in Calcite is zero because we took Calcite as a pure mineral (see Table 1). So the**
126 **underestimation of Mg in dust could be a propagation of errors in previous**
127 **compositions in minerals considered in this study”.**

128

129 Fourthly, and most importantly, the authors use the ratio of the median elemental fraction in
130 model and observations (documented in table 3) to 'tune' their results. This is a quite drastic
131 step, and I wondered what the justification for that step is. I think the authors should give
132 more reasons for this step than just the last line in table 3. Does it bring the models closer to

133 the observations at all measurement sites uniformly? Does it reduce bias? What is the
134 variance ratio between model and data?

135 For the tuning ratio, we aim to bring the models closer to the observations at all measurement
136 globally, i.e. uniformly, so that downstream users (e.g. oceanographers), can use more
137 accurate estimates. From observations, we have found a wide range in fractions of elements in
138 individual site and all sites together, the ratio of the maximum and minimum in measured
139 fractions could reach more than 700 for element K, and more than 200 for Ca and Mn. Using
140 the ratio of averaged ones could introduce a bigger bias. So it is safer to choose a tuning ratio
141 of medians from model and observation to adapt our model result. We add in a discussion of
142 our motivation and the rationale better in the new text in Section 3.4. A better solution
143 would be to solve the problem at the source, of course, which is why we highlight the
144 problem (as discussed in the previous comment by the reviewers). We add text to better
145 explain this point at beginning of Section 3.5.

146

147 And finally, at the present size many the figures resemble more a stamp collection and are
148 almost completely useless to the reader. The authors should think about ways to present their
149 results in a form that allows the reader to have a look without magnifying glasses.

150

151 We have revised the figures to make them more readable. Please note that an additional
152 problem is that the discussion paper uses a square format, while the final paper will have the
153 figures be rectangular, and thus will be larger using the format we use here.

154

155 **3 An incomplete list of typographical, language and other errors**

156 The list of smaller language errors would quite long, and I have therefore not listed
157 minor ones, such as omitted 'the' etc.

158 Page 17497: many errors on this page; one example: line 27, 'calculating' should be
159 'calculation'

160 In updated manuscript the 'calculating' has been changed into 'calculation'.

161

162 Page 17498: What does the sentence 'Here the mineral dependent method is defined
163 as M1' mean? I have no idea.

164 To compare the mineral method with silianpaa method, we define the mineral method as
165 Method 1. For the clarity, we have rewritten this sentence to "**Here the mineral dependent
166 method to calculate soluble element is defined as method 1 (Sol-1). To present
167 uncertainties, the other approach (Method 2, defined as Sol-2) is introduced as reference.
168 It is based on the extractable elemental fraction of in-situ 20µm sieved soil samples,
169 reported by Silianpaa (1982) (Table S1) to combine with FAO soil dataset to get a global
170 soluble elemental inventory independent of soil minerals**".

171

172 Page 17502, lines 4-5: What does the sentence want to say?

173 We mean the global source areas are emitting dust with variable elemental fractions so
174 differentiating in soil elements in source areas in model is necessary and meaningful. We
175 have rewritten this sentence into "**The simulated elemental fractions in dust suggest the
176 differentiating in elements in soils between global source areas is necessary and**

177 **meaningful” to make the clarity.**

178 Page 17502: Many small errors, like missing empty spaces between word, missing

179 word like 'are found (in) dust' Page 17502, lines 23-25: what is a 'relative location'?

180 I don't understand the sentence. The importance of something adds complexity in

181 applying something else?

182 **We have tried to fix the errors listed here and other similar errors in the updated manuscript.**

183 Page 17503, lines 15 ff: 'The monthly variability is calculated by': No, the variability is

184 something that is already defined. I would write 'An index describing montly vaiability..

185 **Yes, the sentence has been changed into “An index describing monthly variability is**

186 **calculated by”.**

187 Page 17504, lines 22-24: Where is the verb in that sentence? Page 17508, lines 16-18:

188 Sentence unclear. Table 2, column 1: textbfAfrica -> **Africa**

189 Here “yielded” is a verb. The sentence of “Due to the high Ca/Al ratio (4.0-10.0) in a range of

190 desert soils in some regions including South Africa, yielded Ca/Al ratios in dust emissions of

191 1.0, being much larger than those from North Africa.” has been changed in “**The high Ca/Al**

192 **ratio (4.0-10.0) in a range of desert soils in some regions including South Africa, yields a**

193 **Ca/Al ratio in dust emissions of 1.0, being much larger than those from North Africa”.**

194

195 Page 17508, lines 16-18 has been changed into “**The Greenland ice sheet accounted for the**

196 **dominant part of receiving elements deposition to ice sheets regions, which is equal to**

197 **the total amount of elements deposited in the whole of the South Atlantic Ocean.”**

198

199 Table 3: Capitalization of words in column 1 needs to be checked

200 Table 4: caption: iffereent -> different

201 footnote b: tunning -> tuning

202 **We have tried our best to fix all the errors listed here and other errors in the updated**

203 **manuscript.**

204

205 Table 5: I don't understand the footnote! Also, the table is much too small to be read

206 Figure 4: Why do the right and left panels have different sizes? Also the colourmap in

207 d) is different from the others. Figure 5: All colorscales are identical! This is probably

208 wrong. Figure 13: The text in the caption is almost un-understanable

209 **For the footnote of Table 5, it means the modeled element deposition has been tuned to adapt**

210 **the model results to the observed element. It is changed into “*Here the soluble element**

211 **deposition using Sol-1 has been tuned by timing tuned ratios (Table 3); Sol-1 refer to**

212 **mineral method after tuning, Sol-2 refer to Sillanpaa method described in the methods**

213 **section (2)” to make it more clear.**

214 **For Figure5, the colorbar scale is identical due to the value means the ratio of the elemental**

215 **fraction in atmospheric dust and dust deposition. It is the same order for all the elements.**

216 **For Figure 13, the caption has been changed into “The percentages of elements in dust**

217 **deposition (%) after tuning. It is tuned based on original percentages of elements in dust**

218 **deposition in Fig. S1 by timing Obs./Mod. ratios listed in Table 3. Si did not change**

219 **because there are not enough observational data available.”**

220

221 **References not already present in the manuscript**

222 Christian, J.R. (2007). Advection in plankton models with variable elemental ratios.

223 Ocean Dynamics, 57(1), 63-71. doi:10.1007/s10236-006-0097-7

224 Nickovic, S., Vukovic, A., and Vujadinovic, M. (2013). Atmospheric processing of iron

225 carried by mineral dust. Atmos. Chem. Phys., 13, 9169–9181, doi:10.5194/acp-13-

226 9169-2013, 2013.

227 **The references above have been cited in the updated manuscript.**

228

229 **Anonymous Referee #2**

230 The paper presents a method of using soil mineral maps to model the elemental content
231 of atmospheric dust. The paper focuses on eight elements (Mg, P, Ca, Mn, Fe, K, Al, and Si),
232 which are mostly of importance for ocean biogeochemistry. The technique represents an
233 attempt to improve upon models that assume fixed fractions for these elements to simulate
234 ocean deposition. This is a daunting task, since gridded soil maps can not capture all of the
235 regional mineralogical variabilities, the range of elemental concentrations in soils and
236 minerals is quite large, and the concentrations of minerals and elements in soils is different
237 than the concentrations of minerals and elements in the atmosphere. Although the description
238 of the model is quite brief in this paper and I am not a modeler, I suspect that many of the
239 model parameterizations required to simulate elemental concentrations in the atmosphere are
240 rudimentary at the present time. Nonetheless, this work is important for evaluating and
241 improving key linkages between soil and atmospheric aerosol composition, and the effect dust
242 deposition on ocean biogeochemistry. I have only minor comments that should be considered
243 before publication.

244 *We thank the reviewer for the very helpful comments, and revise the text to clarify the points
245 addressed by the reviewer. We also agree that this is a first step, and insert a sentence in the
246 conclusions discussing that we think the largest source of uncertainty is in the soil map
247 conversion to elements in the source regions.*

248

249 There are a few spelling errors here and there. For instance, words like fractionsof, dustis, and
250 observedin appear on line 19 of page 12. This may have occurred in the typesetting process,
251 but a spell checker could easily weed out these problems.

252 *Thank you for identifying these typographic and English errors: we have tried to improve the
253 English in the text and correct some errors in the updated manuscript.*

254

255 There are some grammar issues in a few places: line 28 on page 15, line 28 on page 16.
256 Page 7, line 5 and Table 1b: I find it a little odd that the authors are citing "personal
257 communication" with one of the co-authors. Perhaps "unpublished data" would be more
258 appropriate?

259 *Yes, it is already changed into "unpublished data".*

260

261 Pages 8 & 13: SD is never defined. I know that it means standard deviation, but it might
262 be a small barrier for some readers.

263 *SD is defined in the updated manuscript.*

264

265 Page 15, line 23: I don't know that I would say that the model and observations are generally
266 consistent in Figure 10, but then again, I am having a really hard time analyzing such small
267 figures. At first glance, I see a lot of red bars that are much higher than the blue bars. Perhaps
268 a scatter plot with a 1:1 line would be more appropriate for such a comparison? You could use
269 different shapes and colors of the points for the various sites. At any rate, figures are
270 important for "hooking" your readers into reading more, and these small panels will hook few
271 people.

272 As you suggested, we have used the scatter plot to replace the bar figure in the updated
273 manuscript. It is clear the values are close to 1:1 line (most in the range of 2:1 and 1:2 line)
274 for most elements at most sites except for Mg, Mn and Si.

275

276 Figure 2: Way to many world maps for one figure – break it up!

277 We have split Figure 2 to 2 pages to make the size bigger.

278

279 Figure 10: Figure panels are also way too small, and the resulting axes fonts are too small, too.
280 Try to limit yourselves to four panels per figure.

281 Figure 10 has been replotted. Also all the figures in our paper has been reorganized and are
282 much more readable.

283

The list of changes in updated manuscript

We have summarized the changes in the updated version as the below:

1. For the written English, the native English speaking coauthors have helped in rewriting it throughout the manuscript. Please see the following marked up version.
2. For the figures, we have replotted Fig.2, Fig.4-8, Fig.10, Fig.13-15 for the readability. Please see the following marked up version.
3. We have corrected the errors observed by two referees and our own careful review. Please see the following marked up version.
4. Some new sentences and paragraphs have been added in to make the clarity, e.g.:

in section 2.2 *“By splitting the dust into its different mineral elements, we may add additional numerical errors, because the elements are transported separately. There has been considerable work on improving advection algorithms in atmospheric models, and here we use the finite volume advection algorithm as part of the CAM [Lin and Rood, 1997]. While no advection scheme is perfectly mass conserving, monotonic, shape preserving and computationally efficient, this scheme does a good job of balancing these multiple goals and maintaining the strong gradients required in modeling atmospheric constituents (e.g. [Rasch et al., 2006]). Studies focused on elemental distributions in ocean models have suggested the relatively small uncertainties associated with these types of numerical errors (e.g. [Christian, 2007]), and compared with the errors in the source distribution of the minerals, errors from advection are likely to be small and are neglected here.”;*

in section 3.4 *“For this comparison (above), we calculate the elemental fractions and average the fractions temporally for each site and compare to observations, but alternatively, we could average the elemental concentrations and divide by the elemental dust concentrations instead, and this will make a difference in our interpretations. For example, taking site 2-Tazhong, the averaged fraction is 3.5% when we calculate the fractions of iron firstly and average those temporally. However, when we calculate the averaged iron mass and dust mass separately, their ratio is 2.3%. For site3-Yulin, the ratio is 3.6% and 3.1% for the first method and second method, respectively. This difference maybe due to dust storm events. For this comparison, we use the first method, as we think it is more suitable for our goal of simulating the % of each element correctly. “;*

in section 3.5, “Of course, improving our elemental estimates in the source region would be preferred in future studies. From the observations, we have found a wide range in fractions of elements at individual sites and at the sites together; the ratio of the maximum and minimum in measured fractions could reach more than 700 for element K, and more than 200 for Ca and Mn. Because of the limited observations, we use a global tuning factor, based on the median elemental %, and contrast this result with our default modeling approach (Table 3). It is noted that both the median of observed (3.10 %) and modeled (2.9 %) Fe was lower than 3.5%, which was thought to be the fraction of Fe in dust (e.g. Luo et al., 2008; Mahowald et al., 2008).”;

5. Some new reference papers have been added in, e.g.:

Christian, J.R. Advection in plankton models with variable elemental ratios. *Ocean Dynamics*, 57(1), 63-71. doi:10.1007/s10236-006-0097-7, 2007.

Lin, S.-J., and R. B. Rood. An explicit flux-form semi-Lagrangian shallow-water model on the sphere, *Quarterly Journal of the Royal Meteorological Society*, 123, 2477-2498, 1997.

Nickovic S., Vukovic A., Vujadinovic M. (2013). Atmospheric processing of iron carried by mineral dust. *Atmos. Chem. Phys.*, 13, 9169–9181, doi:10.5194/acp-13-9169-2013, 2013.

Rasch, P., D. Coleman, N. Mahowald, D. Williamson, S.-J. Lin, B. Boville, and P. Hess. Characteristics of atmospheric transport using three numerical formulations for atmospheric dynamics in a single GCM framework, *Journal of Climate*, 19, 2243-2266, 2006.

1 **Title:**

2 | **Modeling the Global Emission, Transport and Deposition of Trace Elements** [Associated with Mineral Dust](#)

3 **Authors:**

4 Y. Zhang [yan_zhang@fudan.edu.cn]

5 N. Mahowald [mahowald@cornell.edu]

6 R. A. Scanza [ras486@cornell.edu]

7 | E. Journet [emilie.journet@lisa.u-pec.fr]

8 | K. Desboeufs [karine.desboeufs@lisa.u-pec.fr]

9 | S. Albani [s.albani@cornell.edu]

10 J. F. Kok [jfkok@ucla.edu]

11 | G. Zhuang [gzhuang@fudan.edu.cn]

12 Y. Chen [yingchen@fudan.edu.cn]

13 | D. D. Cohen [dcz@ansto.gov.au]

14 A. Paytan [apaytan@ucsc.edu]

15 M. D. Patey [mpatey@gmail.com]

16 E. P. Achterberg [eachterberg@geomar.de]

17 | J. P. Engelbrecht [Johann.Engelbrecht@dri.edu]

18 K. W. Fomba [fomba@tropos.de]

19

janice 8/10/15 11:23 AM

Deleted: [associated](#)

Unknown

Field Code Changed

Unknown

Field Code Changed

21
22 **Modeling the Global Emission, Transport and Deposition of Trace Elements**
23 **Associated with Mineral Dust**

24 Yan Zhang^{1,2}, Natalie Mahowald², Rachel Scanza², Emilie Journet³, Karine Desboeufs³, Samuel
25 Albani², Jasper F. Kok⁴, Guoshun Zhuang¹, Ying Chen¹, David D. Cohen⁵, Adina Paytan⁶, Matt
26 D. Patey⁷, Eric P. Achterberg^{7,9}, Johann P. Engelbrecht⁸, Khandeh Wadinga Fomba¹⁰

- 27 1. Shanghai Key Laboratory of Atmospheric Particle Pollution and Prevention (LAP³), Department of Environmental
28 Science and Engineering, Fudan University, Shanghai, China
- 29 2. Department of Earth and Atmospheric Science, Cornell University, Ithaca, NY, USA
- 30 3. LISA, UMR CNRS 7583, Université Paris-Est Créteil et Université Paris-Diderot, Créteil, France
- 31 4. Department of Atmospheric and Oceanic Sciences, University of California, Los Angeles, CA, USA
- 32 5. Australian Nuclear Science and Technology Organization, Locked Bag 2001, Kirrawee DC, NSW, 2232, Australia
- 33 6. Earth and Planetary Sciences Department, University of California, Santa Cruz, CA 95064, USA.
- 34 7. Ocean and Earth Science, National Oceanography Centre Southampton, University of Southampton, Southampton
35 SO14 3ZH, UK
- 36 8. Desert Research Institute (DRI), 2215 Raggio Parkway, Reno, Nevada 89512-1095, USA
- 37 9. GEOMAR, Helmholtz Centre for Ocean Research, 24148 Kiel, Germany
- 38 10. Leibniz Institute for Tropospheric Research (TROPOS), 04318 Leipzig, Germany.
- 39

40 **Abstract** Trace element deposition from desert dust has important impacts on ocean primary
41 productivity, [the quantification of which could be useful in determining the magnitude and sign of the](#)
42 [biogeochemical feedback on radiative forcing](#). However, [the impact of elemental deposition to remote ocean](#)
43 [regions is not well understood and is not currently included in global climate models](#). In this study, emission
44 inventories for [eight elements](#), primarily of soil origin, Mg, P, Ca, Mn, Fe, K, Al, and Si [are](#) determined based
45 on a global mineral dataset and a soil dataset. [The resulting elemental fractions are](#) used to drive the desert dust
46 model in the Community Earth System Model (CESM) in order to simulate the elemental concentrations of
47 atmospheric dust. Spatial variability of mineral dust elemental fractions [is](#) evident on a global scale,
48 particularly for Ca. Simulations of global variations in the Ca/Al ratio, which typically range from around 0.1
49 to 5.0 in soils, [are](#) consistent with observations, suggesting [that this ratio is a good signature for dust source](#)
50 regions. The simulated variable fractions of chemical elements are sufficiently different, estimates of
51 deposition should include elemental variations, especially for Ca, Al and Fe. The model results have been
52 evaluated with observations [of elemental aerosol concentrations](#) from desert regions and dust events in
53 non-dust regions, providing insights into uncertainties in the modeling approach. The ratios between modeled

Rachel Scanza 8/8/15 10:36 AM

Deleted: a

Rachel Scanza 8/8/15 10:36 AM

Deleted: S,

Rachel Scanza 8/8/15 10:48 AM

Deleted: .

Rachel Scanza 8/8/15 10:52 AM

Deleted: 8

Rachel Scanza 8/8/15 10:42 AM

Deleted: , which are

Rachel Scanza 8/8/15 10:42 AM

Deleted:

janice 8/10/15 4:57 PM

Deleted: were

Rachel Scanza 8/8/15 10:41 AM

Deleted: s

Rachel Scanza 8/8/15 10:53 AM

Deleted: Datasets of

janice 8/10/15 4:57 PM

Deleted: were

janice 8/10/15 4:57 PM

Deleted: was

janice 8/10/15 4:57 PM

Deleted: d

Rachel Scanza 8/8/15 10:56 AM

Deleted: sources

janice 8/10/15 4:57 PM

Deleted: were

Cornell University 8/6/15 12:16 PM

Deleted: to be

Rachel Scanza 8/8/15 10:57 AM

Deleted: rent that

Rachel Scanza 8/8/15 10:57 AM

Deleted: nal

Rachel Scanza 8/8/15 10:58 AM

Deleted: data

72 and observed elemental fractions range from 0.7 to 1.6, except for Mg and Mn (3.4 and 3.5, respectively).
73 Using the soil database improves the correspondence of the spatial heterogeneity in the modeling of several
74 elements (Ca, Al and Fe) compared to observations. Total and soluble dust element fluxes to different ocean
75 basins and ice sheet regions have been estimated, based on the model results. Annual inputs of soluble Mg, P,
76 Ca, Mn, Fe and K associated with dust using the mineral dataset are 0.28 Tg, 16.89 Gg, 1.32 Tg, 22.84 Gg,
77 0.068Tg, and 0.15 Tg to global oceans and ice sheets.

79 **Key word:** dust; Ca/Al ratio; dust; minerals; atmospheric deposition; global model

80 **1 Introduction**

81 Desert dust aerosols are soil particles suspended in the atmosphere by strong winds, and originate primarily
82 from regions with dry, un-vegetated soils. Desert dust particles are thought to contain several important
83 chemical elements, which can impact the earth system by influencing biogeochemical cycles, in particular,
84 marine primary productivity (Martin et al., 1991; Duce and Tindale, 1991; Herut et al., 1999, 2002, 2005; Okin
85 et al., 2004; Jickells et al., 2005). Iron (Fe) is considered the most important element carried in dust, and low
86 Fe supplies combined with a low dust solubility are thought to limit phytoplankton growth in High Nutrient
87 Low Chlorophyll (HNLC) regions. The HNLC regions feature residual macronutrient (e.g. nitrogen (N) and
88 phosphorus (P)) concentrations, but productivity remains limited by the low supply of Fe (e.g. Martin et
89 al., 1991; Boyd et al., 1998). Further studies have linked Fe to the nitrogen cycle because of high Fe
90 requirements of N fixing organisms (e.g. Capone et al., 1997). While there are internal sedimentary sources of
91 Fe in the ocean, dust deposition is an important source of new Fe to remote regions of the ocean (e.g. Fung et
92 al., 2000, Lam and Bishop, 2008; Moore and Braucher, 2008). Desert dust also contains P, which is a limiting
93 nutrient in some ocean and land regions (e.g. (Mills et al., 2004; Okin et al., 2004; Swap et al., 1992)),
94 especially on longer time scales. In addition, as a dominant constituent of mineral dust, silicon (Si) is an
95 important nutrient for diatoms which are central in ocean productivity (Morel et al., 2003). Other elements
96 released from mineral dust which may be important for ocean biogeochemistry including manganese (Mn) as a
97 biologically essential nutrient and aluminum (Al) as a tracer of atmospheric inputs (e.g. Nozaki, 1997;
98 <http://www.geotraces.org/science/science-plan>).

99 Previous studies have emphasized the importance of measuring elemental composition of dust elements
100 (Kreutz and Sholkovitz, 2000; Cohen et al., 2004; Marino et al., 2004; Marteel et al., 2009), and there are a
101 range of studies highlighting observations of elemental distributions and ecosystem impacts (e.g. Baker et al.,
102 2003; Herut et al., 2002; Buck et al., 2006; Paytan et al., 2009; Chen and Siefert, 2004; Measures and Vink,
103 2000). In-situ observations show evidence of heterogeneities in elemental fractions over arid soil regions
104 (Svensson et al., 2000; Zhang et al., 2003; Shen et al., 2005, 2006; Li et al., 2007). Ratios between elements
105 including Si, Al, Mg, Ca, and in particular Ca/Al ratios have also been used to distinguish dust source regions,

- janice 8/10/15 4:58 PM
Deleted: d
- Rachel Scanza 8/8/15 11:15 AM
Deleted:
- Rachel Scanza 8/8/15 11:15 AM
Deleted: for Mg and Mn, respectively.
- Rachel Scanza 8/8/15 11:16 AM
Deleted:
- janice 8/10/15 4:58 PM
Deleted: improved
- Rachel Scanza 8/8/15 11:18 AM
Deleted: associated
- Rachel Scanza 8/8/15 11:19 AM
Deleted: int
- Rachel Scanza 8/8/15 11:18 AM
Deleted: s
- janice 8/10/15 4:58 PM
Deleted: were
- Rachel Scanza 8/8/15 11:21 AM
Deleted: principally
- Rachel Scanza 8/8/15 11:22 AM
Deleted: , and
- Rachel Scanza 8/8/15 11:22 AM
Deleted: ly
- Cornell University 8/6/15 10:55 AM
Deleted: ,1991
- Cornell University 8/6/15 10:55 AM
Deleted: ,
- Rachel Scanza 8/8/15 11:23 AM
Deleted: so-called
- Rachel Scanza 8/8/15 11:24 AM
Deleted: low because
- Rachel Scanza 8/8/15 11:24 AM
Deleted: of
- Rachel Scanza 8/8/15 11:26 AM
Deleted: ,

124 for example the Asian desert (Zhang et al., 1996; Sun et al., 2005; Han et al., 2005; Shen et al., 2007) and
125 African deserts (Bergametti et al., 1989; Formenti et al., 2008).

126 Xuan (2005) has simulated the emission inventory of trace elements in the dust source regions of East Asia.
127 However, there has not yet been a study to model the distribution of dust-associated elements on a global scale.
128 Global dust models usually assume a fixed fraction (e.g. normalized to Al) of each element in dust to simulate
129 global dust elemental transport and deposition. For example, Fe is thought to contribute 3.5% and P 0.075% to
130 mineral dust (by mass) (e.g. Luo et al., 2008; Mahowald et al., 2008). Besides spatial variations in elemental
131 compositions, particle size distribution forms another important determinant of elemental abundance in
132 deposited dust. Depending on the particle size distribution, trace elements may remain more or less suspended
133 in the atmosphere and deposited by dry or wet deposition at various distances from desert regions (Seinfeld
134 and Pandis, 1998). There have been very few studies investigating particle size distribution and elemental
135 concentrations in soil and dust by direct measurement (Schütz and Rahn, 1982; Reid et al., 2003; Castillo et al.,
136 2008; Engelbrecht et al., 2009a,b), and even fewer modeling studies have included this. The ability to model
137 the deposition of specific elements associated with dust in global simulations has been hindered by a lack of
138 understanding of the spatial and temporal variability, as well as the particle size distribution associated with
139 different dust sources. As noted by Lawrence and Neff (2009), it seems most appropriate to use a globally
140 averaged value of dust composition to estimate the elemental flux from dust, given the lack of direct
141 measurements of the spatial distribution of elements in dust. However, the use of a global mineral map
142 (Claquin et al., 1999; Nickovic et al. 2012, 2013; Journet et al., 2014) and chemical compositions of minerals
143 (Journet et al., 2008) allows us to simulate global elemental inventories from mineral soils, which could be
144 used in a global dust model.

145 This study aims to introduce a technique to determine a size-fractionated global soil elemental emission
146 inventory based on two different datasets, a global soil dataset and a mineralogical dataset. A companion paper
147 evaluates the ability of the model to simulate mineralogy and the impact on radiation (Scanza et al., 2015). The
148 elemental emission dataset estimated for Mg, P, Ca, Fe, Mn, K Al, and Si was used as an input to a model
149 simulation of the global dust cycle to present the elemental distributions, which were compared against
150 available observations of concentration and deposition to different ocean regions. Our goal is to assess the
151 variability of elemental fractions in atmospheric and deposited dust, and to investigate whether the elemental
152 emission dataset can adequately predict this variability. This study focuses on desert dust particles, and thus
153 disregards other potentially important sources of the elements such as combustion processes (e.g. Guieu et al.,
154 2005; Luo et al., 2008; Mahowald et al., 2008). We focus on total elemental concentrations, but discuss two
155 methodologies for soluble metal distributions from soil emissions. We also do not consider any atmospheric
156 processing, which is likely to be important for some chemical components (e.g. Mahowald et al., 2005; Baker
157 and Croot, 2010).

159 2 Materials and Methods

Rachel Scanza 8/8/15 11:30 AM

Deleted: for

Rachel Scanza 8/8/15 11:31 AM

Deleted:

Rachel Scanza 8/8/15 11:32 AM

Deleted: , and

Rachel Scanza 8/8/15 11:32 AM

Deleted: f

Rachel Scanza 8/8/15 11:36 AM

Deleted: relate this to

Rachel Scanza 8/8/15 11:37 AM

Deleted: ese phenomena

Cornell University 8/6/15 10:55 AM

Deleted: ,1999

Cornell University 8/6/15 10:56 AM

Deleted: ; Journet

Cornell University 8/6/15 10:56 AM

Deleted: minerals(

Cornell University 8/6/15 10:56 AM

Deleted: 2008)allows

Rachel Scanza 8/8/15 11:41 AM

Deleted: a

Rachel Scanza 8/8/15 11:41 AM

Deleted:

Rachel Scanza 8/8/15 11:42 AM

Deleted: s

Rachel Scanza 8/8/15 11:40 AM

Deleted: 4

janice 8/10/15 10:28 AM

Deleted: ,

Rachel Scanza 8/8/15 11:49 AM

Deleted: , estimated for Mg, P, Ca, Fe, Mn, K Al, and Si

Rachel Scanza 8/8/15 11:47 AM

Deleted:

178 2.1 Soil and mineral datasets

179 The soil map of the world used in this study comes from the Food and Agriculture Organization (FAO) of
180 the United Nations soils dataset, and includes 136 soil units [FAO-United Nations Educational, Scientific, and
181 Cultural Organization (FAO-UNESCO, 1995) at a 5-minute resolution. The global dataset of soil clay and silt
182 data are used in this study. Following Claquin et al. (1999) and Nickovic et al. (2012), the illite, hematite,
183 kaolinite, smectite, quartz, feldspars, calcite and gypsum contents are specified for different clay and silt soil
184 types, and the global mineral distribution is presented in Scanza et al (2015). Some minerals found in dust such
185 as dolomite were not considered by Claquin et al. (1999) and Nickovic et al. (2012) and have also been
186 disregarded in this study due to the lack of data on their distribution.

187 The elemental compositions of hematite and aluminosilicate minerals used in this study are taken from
188 previous works (Journet et al. (2008) and unpublished data provided by E. Journet, 2012) and were obtained by
189 X-ray fluorescence spectrometry (XRF) (Table 1a). Most of minerals used by Journet et al. (2008) are
190 reference materials from the Society's Source Clays Repository, i.e. hematite, illite, kaolinite, montmorillonite.
191 The elemental compositions obtained by XRF are in the range of published values for these reference materials
192 (e.g. Mermut and Cano, 2001; Gold et al., 1983), validating the obtained composition for the unreferenced
193 materials. Moreover, the purity of all minerals samples is estimated by X-Ray diffraction. Note that the
194 mineralogical maps used in this study do not distinguish feldspar and smectite subtypes. For feldspars, the
195 elemental composition is mostly averaged based on 2 subtype minerals: orthoclase (potassic feldspar) and
196 oligoclase (sodium-calcium feldspar). For smectites, the montmorillonite subtype is the most commonly
197 identified smectite in desert dust, particularly for Saharan dust e.g. Goudie and Middleton, 2006). The
198 chemical composition of montmorillonite is used in this study as an analog for smectite. For calcite, gypsum,
199 and quartz, the natural minerals could contain substitutions or impurities from clays, which are
200 variable depending on origin, formation, contamination, etc. of minerals. Because regional silt samples were
201 not available for spectroscopy, we use the theoretical composition of elements in calcite, gypsum and quartz
202 (Table 1a). The mass fraction of Ca in calcite (CaCO_3) and gypsum ($\text{CaSO}_4 \cdot 2\text{H}_2\text{O}$) are taken as 40% and
203 23.3%, respectively. A mass fraction of 46.7% Si is used for pure quartz (SiO_2).

204 Following the total element calculation, soluble elemental fractions are estimated based on soluble elemental
205 contents of minerals at pH=2 reported by Journet et al (2008) for hematite and the aluminosilicates, and is
206 listed in Table 1b. The fractional solubility of Ca in calcite and gypsum used is 7% and 0.56%, respectively,
207 and that of Si in quartz was 0.0003% based on individual solubility product (K_{sp}) at pH=2 (Petrucci et al.,
208 2001). Here the mineral dependent method used to calculate soluble elements is defined as Method 1 (Sol-1).
209 To present uncertainties, another approach (Method 2, defined as Sol-2) is introduced as a reference. It is based
210 on the extractable elemental fractions of in-situ 20 μm sieved soil samples reported by Sillanpaa (1982) (Table
211 S1) and is combined with an FAO soil dataset to get a global soluble elemental inventory independent of soil
212 minerals. It is noted that there is no detailed size distribution for soil samples in M2. Thus, the fractions of
213 soluble elements in clay and silt are assumed to be equal to that of the bulk soils themselves.

janice 8/10/15 4:59 PM
Deleted: came ...omes from the Food ... [1]

Rachel Scanza 8/8/15 11:54 AM
Deleted: smectite

janice 8/10/15 5:00 PM
Deleted: were

Rachel Scanza 8/8/15 11:52 AM
Deleted: 4

janice 8/10/15 5:00 PM
Deleted: were

yanzhang 8/2/15 2:49 PM
Deleted: personal communication

Cornell University 8/6/15 12:22 PM
Deleted: It is noted...ote that the actu ... [2]

Rachel Scanza 8/8/15 12:02 PM
Deleted: s...and smectites...subtypes ... [3]

Cornell University 8/6/15 12:22 PM
Deleted: so

Rachel Scanza 8/8/15 11:58 AM
Deleted: gous...forof ... [4]

Cornell University 8/6/15 12:22 PM
Deleted: typically

Rachel Scanza 8/8/15 12:05 PM
Deleted: as...clays, which are ... [5]

yanzhang 8/2/15 2:36 PM
Deleted: ting

janice 8/10/15 5:01 PM
Deleted: were

Rachel Scanza 8/8/15 12:16 PM
Deleted: the ...ematite and the ... [6]

yanzhang 8/2/15 2:37 PM
Deleted: (M2)

Rachel Scanza 8/8/15 12:25 PM
Deleted: ...reported by Silli ... [7]

yanzhang 8/2/15 2:38 PM
Deleted: B

Cornell University 8/6/15 12:23 PM
Deleted: to

Rachel Scanza 8/8/15 12:27 PM
Deleted: soil

Cornell University 8/6/15 12:24 PM
Deleted: the one in

280 | Table S1 Averaged macronutrient contents (%) of soils classified by FAO/Unesco soil units *

281 | One drawback of our approach is that we disregard the large variability of soils included within each defined
282 | “soil type”. The range of minerals within each soil type is large (e.g. Claquin et al., 1999), and the range of
283 | elemental concentrations in each mineral is also large (Journet et al., 2008). The resolution of our model is
284 | such that despite the actual heterogeneity of soils at a particular location, we prescribe an average at each
285 | gridbox, which tends to reduce the variability in elemental composition in the mineral dust in the atmosphere.

286 | This is likely to be the largest source of uncertainty in our approach.

287 | Table 1 (a) Generalized mineral compositions (%) applied in this study ;(b) Elemental solubility as a percentage of
288 | the element contained in the minerals (%)

289 | Table 2 Emission rates (Tg/yr) and percentages of elements over desert regions (%)
290

291 2.2 Numerical Model description

292 | Community Earth System Model version 1.0.3 (CESM1.0.3) is coordinated by the National Center for
293 | Atmospheric Research (NCAR), and has been used to simulate elemental dust emission, transport and
294 | deposition in this study. The bulk mineral aerosol in the Community Atmosphere Model version 4 (CAM4)
295 | was adapted to include eight trace elements within total dust (Scanza et al., 2015). In this model simulation, the
296 | physical scheme CAM4 is driven by the meteorological dataset MERRA, and is simulated spatially at 1.9×2.5
297 | degree resolution for the years 2000-2010. The soil erodibility map used by the dust model has been spatially
298 | tuned (Albani et al., 2014). There are four size classes of dust particles used in the dust emission module in the
299 | bulk scheme with particle diameters of 0.1-1.0, 1.0-2.5, 2.5-5.0 and 5.0-10.0 μm. The sub-bin size distribution
300 | is assumed to follow a log-normal distribution with a mass median diameter of 3.5 μm (Mahowald et al., 2006)
301 | and a geometric standard deviation of 2.0 μm (Zender et al., 2003). Combining these log-normal parameters
302 | with the brittle fragmentation theory of dust emission (Kok, 2011) yields each bin’s partitioning of dust aerosol
303 | mass between the soil’s clay and silt size fractions (see Table B3 and Scanza et al., 2015). The elements in the
304 | dust undergo three-dimensional transport individually in each of the different size bins, identically to bulk dust
305 | in the original model. Elemental atmospheric mixing ratios, and wet and dry deposition are updated at each
306 | model time step based on actual elemental fields and the corresponding tendencies.

307 | By splitting the dust into its different mineral elements, we may add additional numerical errors, because the
308 | elements are transported separately. There has been considerable work on improving advection algorithms in
309 | atmospheric models, and here we use the finite volume advection algorithm as part of the CAM [Lin and Rood,
310 | 1997]. While no advection scheme is perfectly mass conserving, monotonic, shape preserving and
311 | computationally efficient, this scheme does a good job of balancing these multiple goals and maintaining the
312 | strong gradients required in modeling atmospheric constituents (e.g. [Rasch et al., 2006]). Studies focused on
313 | elemental distributions in ocean models have suggested the relatively small uncertainties associated with these
314 | types of numerical errors (e.g. [Christian, 2007]), and compared with the errors in the source distribution of
315 | the minerals, errors from advection are likely to be small and are neglected here.

yanzhang 8/2/15 2:39 PM

Deleted: B

Cornell University 8/6/15 10:56 AM

Deleted:)of

Rachel Scanza 8/8/15 12:35 PM

Deleted: Our models apply averages,

Cornell University 8/6/15 10:56 AM

Deleted: Table1(

Cornell University 8/6/15 10:56 AM

Deleted: b)Elemental

Rachel Scanza 8/8/15 12:36 PM

Deleted: 4

janice 8/10/15 5:01 PM

Deleted: was

janice 8/10/15 5:01 PM

Deleted: was

Rachel Scanza 8/8/15 1:00 PM

Deleted: and referedreferred to

Rachel Scanza 8/8/15 1:00 PM

Deleted: were

janice 8/10/15 5:02 PM

Deleted: was

Rachel Scanza 8/8/15 1:02 PM

Deleted: 4

Rachel Scanza 8/8/15 1:03 PM

Deleted:

Cornell University 8/6/15 10:08 AM

Formatted: Font:(Default) Times New Roman, 10.5 pt

Cornell University 8/6/15 10:08 AM

Formatted

... [9]

Cornell University 8/6/15 10:08 AM

Formatted

... [8]

Cornell University 8/6/15 10:08 AM

Formatted

... [10]

Cornell University 8/6/15 10:08 AM

Formatted

... [11]

Cornell University 8/6/15 10:08 AM

Formatted

... [12]

Cornell University 8/6/15 10:08 AM

Formatted

... [13]

Cornell University 8/6/15 10:08 AM

Formatted

... [14]

Cornell University 8/6/15 10:08 AM

Formatted

... [15]

Cornell University 8/6/15 10:08 AM

Formatted

... [16]

Cornell University 8/6/15 10:08 AM

Formatted

... [17]

329 | Table S2. The fraction of dust aerosol mass contributed by the soil clay and silt fractions for each of the 4 particle size
330 | bins for the bulk scheme in CAM4.
331

332.3 Observational data

333 | An element dataset of ground based aerosol measurements at 17 sites (Table B3) js used to evaluate the
334 | elemental dust simulation (Sun et al., 2004a,b; Wang et al., 2010; Chen et al., 2008; Engelbrecht et al., 2009;
335 | Carpenter et al., 2010; Cohen et al., 2011; Guo et al., 2014; Formenti et al., 2008; Desboeuufs et al., 2010). The
336 | sites are close to major dust-producing regions (Figure 1), including 10 Asian sites (Central Asia: Hetian,
337 | Tazhong; East Asia: Yulin, Duolun, Shengshi; South Asia: Hanoi, and Marnila; Middle East: Balad, Baghdad,
338 | Taji), 5 African sites (West Africa: Cape Verde Atmospheric Observatory (CVAO); East Africa: Eilat; North
339 | Africa: Tamanrasset, Banizoumbou, and Douz), and 2 Australian sites (Muswellbrook, Richmond). Generally,
340 | these field aerosol samples (Total Suspended Particulates (TSP), PM₁₀, PM_{2.5}) have 1-3 day collection periods
341 | during the period 2001-2010, and were chemically analyzed for elemental composition. No observational
342 | aerosol mass concentrations at the Cape Verde station could be used in this study. At this site, the particulate,
343 | matter (PM) concentrations are estimated by assuming an Al to total dust mass ratio of 0.0804. In order to be
344 | certain that only desert dust elements are compared with the model results, only data collected during dust
345 | storm seasons are selected. Measurement sites from which data are taken are listed in Table B3, which includes
346 | related methodological details.

347 | In addition, the dataset of dust deposition at more than 100 sites worldwide js used to evaluate modeled dust
348 | deposition fluxes (Albani et al., 2014).

349 | **Fig.1. Observational sites** (S1-Hetian, China; S2-Tazhong, China; S3-Yu Lin, China; S4-Duolun, China;
350 | S5-Shengsi, China; S6-Hanoi, Vietnam; S7-Marnila, Philippines; S8- Balad, Iraq; S9-Balad, Iraq; S10-Taji, **Iraq**;
351 | S11-Eilat; S12-Cape Verde Atmospheric Observatory (CVAO); S13-Muswellbrook, Australia; S14-Richmond,
352 | Australia; S15-Tamanrasset, Algeria; S16-Banizoumbou, Niger; S17-Douz, Tunisia) **and dust-producing regions**
353 | (WAsia: West Asia; NC-As: **North** Central Asia; CAsia: **Central** Asia; SC-As: South Central Asia; EAsia: East Asia;
354 | WN-Af: North West Africa; EN-Af: North East Africa; S-NAf: Southern North Africa; SAf: Southern Africa;
355 | **MNWAm**: Middle North West America; **SNWAm**: Southern North West America; SAmI: Northern South America;
356 | SAm2: Southern South America; WAus: West Australia; EAus: East Australia)

357 | Table S3. Locations of 17 sampling sites

358 | 3 Results and Discussion

359 | 3.1 Fractions of element in arid soil regions

360 | The global distributions of the elements Mg, P, Ca, Mn, Fe, K, Al, and Si in bulk soils as mass percentages
361 | in soils are presented in Fig. 2.

362 | 3.1.1 Global mapping of soil associated elements

zhang yan 8/2/15 8:42 PM
Deleted: B2

janice 8/10/15 5:02 PM
Deleted: was

Rachel Scanza 8/8/15 3:29 PM
Deleted: across the world as shown in

Rachel Scanza 8/8/15 3:29 PM
Deleted: .

Rachel Scanza 8/8/15 3:30 PM
Deleted: the observation sites

Rachel Scanza 8/8/15 3:30 PM
Deleted: e

Rachel Scanza 8/8/15 3:31 PM
Deleted: nents

Rachel Scanza 8/8/15 3:31 PM
Deleted: e

janice 8/10/15 5:02 PM
Deleted: were

Rachel Scanza 8/8/15 3:32 PM
Deleted: s

janice 8/10/15 5:02 PM
Deleted: were

janice 8/10/15 5:02 PM
Deleted: were

janice 8/10/15 5:03 PM
Deleted: was

Cornell University 8/6/15 10:58 AM
Deleted: ,Iraq

Cornell University 8/6/15 10:58 AM
Deleted: :North

Cornell University 8/6/15 10:58 AM
Deleted: :Central

Rachel Scanza 8/8/15 3:34 PM
Deleted: MWNAm

Rachel Scanza 8/8/15 3:34 PM
Deleted: SWNAm

Cornell University 8/6/15 10:58 AM
Deleted: i

janice 8/7/15 8:55 PM
Deleted: B3

383 Fractions of elements in soils vary between mineralogical clay and silt fractions. Spatial variability of soil
 384 chemistry is seen on a global scale (Fig.2). A large range of variability for some elements within one given
 385 source region is observed (e.g. Ca, Fe, Mn, Al). The most extreme variability is observed for Ca in soil silt,
 386 which varied from 0.5 to 34.3%, and is much higher in West and Central Asia, South Africa and Northern
 387 South America than in other parts in the world. This is ascribed to the presence of feldspar and gypsum, both
 388 being important source minerals for Ca in these regions. In Central and East Asia, the Ca content increased
 389 from east to west, showing a similar spatial trend to that reported by Xuan et al. (2005). A south to north
 390 gradient of Ca content was also observed in the Sahara following the carbonate distribution of soils (Kandler et
 391 al., 2007; Formenti et al., 2011). In southern North Africa, South Africa and the Western Australia, clay soil
 392 and fine dust emissions have higher Al and P concentrations than elsewhere. In Eastern Australia, Patagonia,
 393 and the northern South Africa, the Fe content of soils is also higher than in other regions. Due to their high
 394 content of quartz, soils generally have 25-40% Si. These elemental distributions are in agreement with other
 395 published data for Fe, as they are derived from similar regions (e.g. Claquin, 1999; Hand, 2004).

396 Fig.2 Global elemental distributions (in mass percentage) in a1: Clay Mg, a2: Clay P, a3: Clay Ca, a4: Clay Mn, a5: Clay
 397 Fe, a6: Clay K, a7: Clay Al, a8: Clay Si; b1: Silt Mg, b2: Silt P, b3: Silt Ca, b4: Silt Mn, b5: Silt Fe, b6: Silt K, b7: Silt Al,
 398 b8: Silt Si.

399 3.1.2 Elemental composition of soils and airborne dust

400 Trace elements in soils show different associations with particle size patterns depending on the size
 401 distribution of soil minerals. For example, Mg, P, Fe, Mn, and Al are dominant in the clay size fraction (< 2
 402 µm) (Fig. 3b). Fractions of Al and Fe reach 11.7% and 3.1% in clay fractions of soils, while only 2.8% and 1.2%
 403 in silt fractions of soils, respectively. However, Ca and Si show a slight enrichment in coarser soil fractions. Ca
 404 comprises 2.6% of soils in the clay fraction, but 3.6% in the soil silt fractions. This is consistent with the size
 405 distribution of Ca and Fe-rich individual particle groupings measured in Saharan dust (Reid et al., 2003). K has
 406 nearly equal distributions in clay and silt fractions of soils. Taking the fractions of elements in soils as inputs,
 407 the fractions of elements in dust emission can be predicted. Our classification of soil particles into four aerosol
 408 sizes (Table B2) provides heterogeneity in elements across sizes, but allows for a mixing across soil sizes,
 409 reducing the differences among size fractions. For example, the percentage of Fe remains unchanged from clay
 410 soil to fine mode dust emission, but changes substantially from silt soil (1.2%) to coarse mode dust (2.2% in
 411 Bin 3). A similar pattern appears for the other elements, and the differences between elemental percentages
 412 in the soils are reduced when dust emissions are considered (Fig. 3a vs. 3b).

413 Fig.3 Global mean elemental percentages in (a) four-bin dust emission and (b) clay and silt fractions of soils (Bin1-4 refer to
 414 particle range listed in Table S2, clay refer to < 2µm, silt refer to > 2µm)

415 3.1.3 Elemental dust emissions over desert regions

416 Annual elemental dust emissions over 15 dust-producing regions (shown in Fig.1) are determined (Table 2).
 417 The annual average of total global dust emission is estimated to be 1582 Tg based on 2001-2010 simulations,

janice 8/10/15 5:03 PM
 Deleted: varied

Cornell University 8/6/15 12:26 PM
 Deleted: demonstrated

janice 8/10/15 5:03 PM
 Deleted: was ...s much higher in W... [18]

zhang yan 8/2/15 8:43 PM
 Formatted: Font:9 pt, Bold, (Asian) Chinese (PRC)

zhang yan 8/2/15 8:43 PM
 Deleted: (a) clay fraction of soils and (b) silt fraction of soils -

janice 8/10/15 5:04 PM
 Deleted: ed

Rachel Scanza 8/8/15 3:38 PM
 Deleted: , e.g.

janice 8/10/15 5:04 PM
 Deleted: were

Rachel Scanza 8/8/15 3:39 PM
 Deleted:

janice 8/10/15 5:04 PM
 Deleted: ed

Rachel Scanza 8/8/15 3:39 PM
 Deleted: is...2.6% of soils in their... [19]

janice 8/10/15 5:05 PM
 Deleted: remained ...emains unchar... [20]

Cornell University 8/6/15 12:28 PM
 Deleted: where ...nd the differences ... [21]

janice 8/10/15 5:05 PM
 Deleted: is

Cornell University 8/6/15 12:29 PM
 Deleted: in the

janice 8/7/15 8:54 PM
 Deleted: B2

janice 8/10/15 5:06 PM
 Deleted: were ...re determined (Tab... [22]

464 and js within the wide range (514 to 5999 Tg/yr) as reported by previous studies (e.g. Textor et al., 2006,
 465 2007; Prospero et al., 2010; Huneus et al., 2011). Africa and Asia account for 68% and 31% of the global
 466 emissions, respectively. Correspondingly, trace element emissions are dominant from African desert regions,
 467 with percentages ranging between 65%-70%. Specifically, Al emission from Africa account for 70% of global
 468 Al emissions, of which 64% originated from the Western Sahara. For Asian desert regions, elemental dust
 469 account for 29-34% of the global total amount, with Ca being the strongest contributor (34%) to global Ca
 470 emissions. The percentage of Fe is similar to Al in the total dust emissions with 67% and 32% of Fe from
 471 Africa and Asia, respectively. The maximum % element for Ca at 5% was in dust emission from West Asia,
 472 being more than 4 times higher than Southern North Africa (1.2%). However, the fraction of Al and Si is
 473 largest in dust emission from Southern North Africa, with values of 9.0% and 31%, respectively. The fractions
 474 of Fe and P are 2.8%, and 0.08% in Australia, which is higher than that in other source regions. The simulated
 475 elemental fractions in dust suggest that differentiating elements in soils between global source areas is
 476 necessary and meaningful.

477 **Table 2 Emission rates (Tg/yr) and elemental composition of dust over desert regions (%)**

478

479 3.2 Spatial and seasonal distribution in fractions of elements in atmospheric and deposited 480 dust

481 3.2.1 Elemental fractions in global atmospheric dust and deposited dust

482 The modeled fractions of different elements in atmospheric dust have substantial spacial variability (Fig. 4). Fe
 483 content is greater than 2% for most regions, with a global mean of 2.7% in atmospheric dust. The maximum
 484 contributions of Fe, Al, P and Mn fractions are observed in the tropical Pacific region with values greater than
 485 3%, 10%, 0.08%, and 0.02%, respectively. For Ca, Si and K, a higher fraction is evident in terrestrial
 486 environments. There are obvious land-ocean gradients existing in the distributions of elemental fractions, with
 487 higher Ca and Si fractions in terrestrial regions and higher P, Fe, and Al fractions in oceanic areas, likely due
 488 to their differences in particle size distribution (Fig. 3). There are very similar spatial patterns and magnitudes
 489 shown for the elemental fractions in deposited dust compared with those in atmospheric dust for each element
 490 (Fig. S1, Fig. 5). Higher fractions of Ca and Si in deposited dust is observed in regions close to desert dust
 491 sources where the two elements occur in the coarser size fractions. Conversely, lower Mg, P, Mn, Fe and Al
 492 contents are found in dust deposits close to source regions but higher contents are found over oceans, which is
 493 consistent with the clay soil fraction dominating the finer particle size fractions. The importance of relative
 494 location of the source compared to the deposition to the elemental ratio adds complexity in applying simple
 495 percentages to dust deposition to obtain elemental deposition amounts.

496

janice 8/10/15 5:06 PM
 Deleted: was ...s within the wide ra... [23]

Rachel Scanza 8/8/15 3:46 PM
 Deleted: at ...4%) to global Ca emis... [24]

Cornell University 8/6/15 12:29 PM
 Deleted: to

janice 8/10/15 10:41 AM
 Deleted: contribution ... element fo... [25]

Cornell University 8/6/15 12:30 PM
 Deleted: showed

Rachel Scanza 8/8/15 3:51 PM
 Deleted: the ...ifferentiating in... [26]

yanzhang 8/2/15 2:51 PM
 Deleted: possible...ecessary and an... [27]

Rachel Scanza 8/8/15 3:53 PM
 Deleted: vary substantially on a spatial
 scalespatially

janice 8/10/15 5:07 PM
 Deleted: was ...s evident in terrestri... [28]

Cornell University 8/6/15 12:31 PM
 Deleted: r

Rachel Scanza 8/8/15 3:58 PM
 Deleted: ing...with thosehat...in... [29]

536 Fig.4 Percentages of elements in dust concentration (mass %) : a. Mg, b. P, c. Ca, d. Mn, e. Fe, f. K, g. Al, h. Si.
 537 Elemental % shown here are calculated using the annual mean element concentration divided by the annual mean dust
 538 concentration.

539 Fig.S1 Percentages of elements in deposited dust (%) :a. Mg, b. P, c. Ca, d. Mn, e. Fe, f. K, g. Al, h. Si. Elemental annual
 540 mean % are calculated using the annual mean emission of each element divided by the annual mean emission of dust.

541 Fig.5 Ratio of mass fractions of elements in dust deposition to that in atmospheric dust : a. Mg, b. P, c. Ca, d. Mn, e. Fe, f.
 542 K, g. Al, h. Si. Elemental ratios shown here are calculated using the annual mean element deposition divided by the
 543 annual mean dust deposition.

544
 545 **3.2.2 Seasonal variability of elemental fractions**

546 As described above, the fractions of elements in dust fluctuate temporally and spatially on a global scale. There
 547 are seasonal variations in dust emissions from various desert regions showing different emission patterns
 548 (Fig.S2). The peak periods for dust emissions for various desert regions are consistent with those found by
 549 Werner et al., (2002) (Figure S2). Combining the seasonal cycles in atmospheric dust production with the
 550 element distributions in desert regions, the elemental fractions show large monthly variability, but small
 551 inter-annual variability during 2001-2010 (Fig. A3). Ca and Al have clear seasonal cycles, with Ca having the
 552 largest monthly variability with peak concentrations in the between July and September. This is ascribed to the
 553 higher Ca content of dust originating in West Asia, Central Asia and Southern Africa, regions that provide
 554 large global dust emissions in this period (JJAS). For the other elements, the peak concentrations usually
 555 occurred between March and May (MAM) or November through January (NDJ), corresponding to the periods
 556 when global dust emissions reach a maximum.

557 We modeled the seasonal variability of these elemental fractions. Elemental percentages are calculated using
 558 the climatological monthly mean emission of each element divided by the climatological monthly mean
 559 emission of dust. An index describing monthly variability is calculated by:

$$560 \text{ Monthly variability (\%)} = \frac{SD \text{ of mean fraction}_{month}}{\text{Mean fraction}_{month}} \times 100 \quad (\text{Eq.1})$$

561
 562 Twelve monthly mean fractions are averaged from the ten year simulation, with the corresponding standard
 563 deviations (SDs). Finally, the percentages (Eq.1) of the standard deviation in the monthly means is derived to
 564 describe the variability in elemental fractions of atmospheric dust and deposited dust (Fig. 6 and 7).

565 The monthly mean variation is greatest for Ca, reaching more than 30% variability in some regions. The
 566 temporal variability of elemental percentages in deposited dust tended to be larger than those in atmospheric
 567 dust and show a greater spatial gradient from land to sea. That is similar to the trend of the elemental fractions
 568 in atmospheric and deposited dust (section 3.2.1) since the temporal variation is originally induced by the
 569 spatially variable elemental fraction. In the South Indian Ocean and the South Atlantic Ocean, the monthly

janice 8/7/15 9:06 PM
Formatted: Font:9 pt, Bold, Font color: Auto

janice 8/10/15 5:23 PM
Deleted:

yanzhang 8/2/15 6:15 PM
Deleted: concentration...patterns (F... [30])

Rachel Scanza 8/8/15 4:13 PM
Deleted: is

janice 8/10/15 5:08 PM
Deleted: ed

Rachel Scanza 8/8/15 4:14 PM
Deleted: tions...but small inter-annu... [31]

Cornell University 8/6/15 12:32 PM
Formatted: Font:10.5 pt, Not Bold

Rachel Scanza 8/8/15 4:19 PM
Deleted: %

Cornell University 8/6/15 12:32 PM
Formatted: Font:10.5 pt, Not Bold

Cornell University 8/6/15 12:33 PM
Formatted: Left, Line spacing: single

yanzhang 8/2/15 2:53 PM
Deleted: The

Cornell University 8/6/15 12:33 PM
Formatted: Font color: Black

janice 8/10/15 10:50 AM
Deleted: **Monthly variability (%) =**

janice 8/10/15 10:57 AM
Deleted: -

ras486 8/9/15 3:18 PM
Deleted: Monthly variability %= SD of mean emissionmonth Mean emissionmonthx100 .

janice 8/10/15 5:09 PM
Deleted: were

Rachel Scanza 8/8/15 4:27 PM
Deleted: calculated...from the ten y... [32]

janice 8/10/15 5:09 PM
Deleted: was

Rachel Scanza 8/8/15 4:29 PM
Deleted: shown in

janice 8/10/15 5:09 PM
Deleted: ed...a greater spatial gradi... [33]

626 | variability is even higher and is attributed to the combined effect of variability in dust emissions, spatial
627 | elemental concentration, and dust transport patterns.

628

629 | Fig.S2 Monthly dust emission (kg/m²/s) over 15 dust-producing regions (WAsia: West Asia; NC-As:North Central Asia;
630 | CAsia:Central Asia; SC-As: South Central Asia; EAsia:East Asia; WN-Af:North West Africa; EN-Af: North East Africa;
631 | S-NAf: Southern North Africa; SAF: Southern Africa; MWNAf: Middle North West Africa; SWNAf: Southern North
632 | West Africa; SAM1: Northern South America; SAM2: Southern South America; WAus: West Australia; EAus: East
633 | Australia)

634 | Fig.S3 Seasonal cycle of global mean elemental percentages (%) in atmospheric dust from 2001 to 2010. Elemental % are
635 | calculated using the climatological monthly mean emission of each element divided by the climatological monthly mean
636 | emission of dust.

637
638 | Fig.6 Ten-year monthly variability in mean of elemental percentages in atmospheric dust (mass %) : a. Mg, b. P, c. Ca, d.
639 | Mn, e. Fe, f. K, g. Al, h. Si. Elemental monthly mean % are calculated using the monthly mean emission of each element
640 | divided by the monthly mean emission of dust.

641 | Fig.7 Ten-year monthly variability in mean of elemental percentages in dust deposition (mass %):a. Mg, b. P, c. Ca, d.
642 | Mn, e. Fe, f. K, g. Al, h. Si. Elemental monthly mean % are calculated using the monthly mean emission of each element
643 | divided by the monthly mean emission of dust.

645 | 3.3 Spatial Ca/Al distribution in soils and dust plumes

646 | Of specific interest is the Ca/Al ratio in soil, atmospheric dust and deposited dust as this ratio may be
647 | indicative of specific source regions (Fig. 8). Of all considered ratios, the Ca/Al ratio in soils show the greatest
648 | variability in relation to the relevant desert region (e.g. Formenti et al. (2011)). The Ca/Al ratio ranges mainly
649 | between 0.1-1 in clay fractions of soils and 0.5-5.0 in silt fractions of soils (Fig. 8a,b). The maximum Ca/Al
650 | ratios reaches 160 times the global mean Ca/Al ratio of 1.96 in the silt fraction of soils (Fig. 8b), much higher
651 | than those of other ratios such as Fe, K, and Mn to Al. Asian desert soils have higher Ca/Al ratios, with values
652 | greater than 5 in West Asia and Central Asia. The Ca/Al ratio in dust emissions from Central Asia (1.0-1.6) are
653 | higher than in East Asia (~0.5), which is close to Ca/Al ratios (1.0-1.7) derived from source profiles of Asian
654 | dust (Zhang et al., 1997; Zhang et al., 2003), and also match the observed Ca/Al ratios (0.7-1.3) during Asian
655 | dust events (Sun et al., 2004a,b; Shen et al., 2007). In addition, the Ca/Al ratio in dust emissions in North
656 | Africa are below 0.5, confirming the application of the Ca/Al ratio of 0.3 (or 3.8 with Al/Ca) as an indicator of
657 | North African dust transport to the eastern United States (Perry et al., 1997). Ambient PM_{2.5} dust measured on
658 | the Canary Islands suggests a different ratio (Ca/Al = 1.004) (Engelbrecht et al., 2014). However, this ratio
659 | could be larger for PM₁₀ or TSP. The high Ca/Al ratio (4.0-10.0) in a range of desert soils in some regions
660 | including South Africa, yields a Ca/Al ratios in dust emissions of 1.0, being much larger than those from North
661 | Africa. The modeled spatial pattern of Ca/Al ratio in dust emissions from Asia and northwest Africa is
662 | consistent with the currently available dust pattern compiled by Formenti et al. (2011), but shows relatively
663 | lower values for the Central Asian desert region.

664 | Despite experiencing mixing of airborne dust from various source regions and as a result of dust processing
665 | during transport, the Ca/Al ratios still show spatial variations in global atmospheric dust and deposited dust.
666 | Relative to the Ca/Al ratio in source regions (Fig. 8a,b), the Ca/Al ratio in atmospheric dust over most of
667 | terrestrial Asia ranges between 0.5-0.8, with a maximum of 1.8. This is due to the spatial variability of Ca/Al

janice 8/10/15 5:09 PM
Deleted: was

Rachel Scanza 8/8/15 4:32 PM
Deleted: , ascribed

zhang yan 8/2/15 8:44 PM
Deleted: A

zhang yan 8/2/15 8:44 PM
Deleted: A

janice 8/10/15 5:23 PM
Formatted: Indent: First line: 0 ch

janice 8/10/15 5:09 PM
Deleted: ed...the greatest variability ... [34]

Rachel Scanza 8/8/15 4:34 PM
Deleted: s

janice 8/10/15 5:10 PM
Deleted: had ...ave higher Ca/Al rat ... [35]

Rachel Scanza 8/8/15 4:36 PM
Deleted: ing...the observed Ca/Al r ... [36]

Cornell University 8/6/15 12:33 PM
Deleted: Also

janice 8/10/15 5:11 PM
Deleted: were

Cornell University 8/6/15 12:34 PM
Deleted: There was also the case for a

Rachel Scanza 8/8/15 4:37 PM
Deleted:

janice 8/7/15 9:19 PM
Deleted: (Engelbrecht et al., 2013)

yanzhang 8/2/15 2:54 PM
Deleted: Due to ...t ... [37]

yanzhang 8/2/15 2:58 PM
Formatted: Font color: Red

janice 8/10/15 5:11 PM
Deleted: yielded

yanzhang 8/2/15 2:58 PM
Formatted ... [38]

Rachel Scanza 8/8/15 4:38 PM
Deleted: ing

janice 8/10/15 5:12 PM
Deleted: ed

Rachel Scanza 8/8/15 4:39 PM
Deleted:

janice 8/10/15 5:12 PM
Deleted: ranged

Rachel Scanza 8/8/15 4:39 PM
Deleted: reaching

Cornell University 8/6/15 12:37 PM
Deleted: D

716 | ratio in dust emissions (Fig. 9a) and despite the preferential gravitational settling during transport of silt
717 | fraction which represents the highest Ca/Al variability. The variability in Ca/Al ratio in dust deposited into
718 | oceans and onto ice sheets are also shown in Fig. 9b. Near West Asia and Western Sahara, higher Ca/Al ratios
719 | are noted and the North Indian ocean and Mediterranean sea have a Ca/Al ratio above 0.65 in deposited dust.
720 | As the combined downwind region of central Asia and East Asia, the North Pacific has a Ca/Al ratio around
721 | 0.5. The Ca/Al ratio in dust deposited over the Atlantic ranges between 0.3-0.4 due to the influence of southern
722 | North Africa desert region and East Sahara desert both with low ratios of Ca/Al. Since the soil dataset has a
723 | high spatial resolution of 5 arc minutes (Fig. 8a,b), there is opportunity to increase the model grid resolution
724 | ($1.9 \times 2.5^\circ$ in this study) to a finer resolution. It is expected that Ca/Al ratio will show more spatial
725 | heterogeneity when a finer model resolution is used. We conclude that the Ca/Al ratio can be used to identify
726 | different source areas and the model can be used to support the observations.

728 | **Fig.8 Ca/Al in Soil and ten year averaged Ca/Al ratio in dust emission, concentration and deposition. Top two (a,b) refer**
729 | **to ratio in clay and silt desert soil, middle one (c) refer to ratio in dust emission, and bottom two (d,e) refer to ratio in dust**
730 | **concentration and deposition. Elemental annual mean % are calculated using the annual mean emission of each element**
731 | **divided by the annual mean emission of dust.**

732 | **Fig.9 Ten year averaged Ca/Al ratio in (a) dust emission of source regions and (b) dust deposition into various ocean**
733 | **basins and glaciers. Elemental ratios are calculated using the annual mean emission of Ca divided by the annual mean**
734 | **emission of Al.**

- Cornell University 8/6/15 12:36 PM
Deleted:
- Rachel Scanza 8/8/15 4:41 PM
Deleted: regions
- Rachel Scanza 8/8/15 4:41 PM
Deleted: Close to
- Rachel Scanza 8/8/15 4:42 PM
Deleted: areas
- janice 8/10/15 5:13 PM
Deleted: ranged
- Rachel Scanza 8/8/15 4:44 PM
Deleted: improve the
- Rachel Scanza 8/8/15 4:44 PM
Deleted: of
- Rachel Scanza 8/8/15 4:45 PM
Deleted: degree
- Rachel Scanza 8/8/15 4:45 PM
Deleted:
- Rachel Scanza 8/8/15 4:46 PM
Deleted: a
- Rachel Scanza 8/8/15 4:46 PM
Deleted: -
- zhang yan 8/2/15 8:44 PM
Formatted: Left

3.4 Model evaluation with observational data

The averaged modeled fractions of elements in atmospheric dust at each site for the periods for which observations are available are comparable with observations for most of the sites (Fig. 10a,b). It is clear most scatter values of model and observations are in the range of 2:1 and 1:2 line for most elements in TSP except for Mg, Mn and Si. It shows the emission inventories based on mineralogy and elemental compositions are generally consistent with the available data. A large variability in the % of different elements is observed at the 17 observational sites for most elements, especially for Ca (Fig. 10). The fraction of Fe in the fine mode particle ($PM_{2.5}$) is closer to the observational data than the TSP Fe fraction, implying that Fe in the clay soils is more accurate than that for silt. Since there are only a few reported observations of Si, this element is particularly difficult to verify. Based on averaged elemental fractions in TSP, at 13 sites, the correlation coefficients (R) between modeled and observed fractions range widely (Table 3). Ca and Al had the highest correlations (0.75 and 0.72, respectively). However, the correlation coefficients for P, Mn and K were negative. For Fe, if we neglect the 3 sites in North Africa, the correlation coefficient increases from 0.29 to 0.50. In this area, the observational Fe fractions in TSP are high whereas the modeled ones are low (Fig. 10a,5). The modeled elemental fractions in TSP are close to the observed data, with most ratios ranging between 0.7 and 1.6 (Table 2).

For this comparison (above), we calculate the elemental fractions and average the fractions temporally for each site and compare to observations, but alternatively, we could average the elemental concentrations and divide by the elemental dust concentrations instead, and this will make a difference in our interpretations. For example, taking site 2-Tazhong, the averaged fraction is 3.5% when we calculate the fractions of iron firstly and average those temporally. However, when we calculate the averaged iron mass and dust mass separately, their ratio is 2.3%. For site 3-Yulin, the ratio is 3.6% and 3.1% for the first method and second method, respectively. This difference maybe due to dust storm events. For this comparison, we use the first method, as we think it is more suitable for our goal of simulating the % of each element correctly.

The averaged fractions of Mg and Mn in dust are underestimated by the model at all observational sites. It should be noted that there are some uncertainties when comparing elemental fractions. When the elemental concentration is divided by particle mass concentration to obtain the elemental fraction, the errors are amplified due to error propagation associated with the combination of the error on the particle mass and that of the element concentrations. Even though the available observational data are chosen from source sites or dust events in non-source regions, the contribution from other sources could be important, especially for fine mode particles. The modeled fraction of Mn and Al in fine particles show a larger inconsistency than that those in TSP when compared with observations. Some of the discrepancies may be because the model only includes particles up to 10 μm in diameter, while the observations include larger particle fractions in TSPs. In South Asia, the elemental fractions in dust with the exception of Mn, are always much lower than at another sites, perhaps due to anthropogenic contributions to elemental particulate matter concentrations. In particular, many

- janice 8/10/15 5:45 PM
Deleted: -
- Cornell University 8/6/15 10:32 AM
Deleted: Here we calculate the elemental fractions and average those temporally for each site.
- janice 8/10/15 5:42 PM
Formatted: Indent: First line: 0 cm
- janice 8/10/15 5:48 PM
Deleted: In generally,
- Rachel Scanza 8/8/15 4:47 PM
Deleted: , ...he emission inventories ... [39]
- janice 8/10/15 5:14 PM
Deleted: c... [40]
- Rachel Scanza 8/8/15 4:50 PM
Deleted: that the fraction of Fe is in ... [41]
- janice 8/10/15 5:50 PM
Formatted: Subscript
- janice 8/10/15 5:15 PM
Deleted: d...widely (Table B4 ... [42]
- Rachel Scanza 8/8/15 4:55 PM
Deleted: Icium... and Al had the hig... [43]
- Cornell University 8/6/15 12:39 PM
Deleted: R
- Rachel Scanza 8/8/15 4:58 PM
Deleted: could reach...0.50 from 0.7... [44]
- janice 8/10/15 5:17 PM
Deleted: e...l ... [45]
- Rachel Scanza 8/8/15 4:56 PM
Deleted: e l... The modell...d elemen... [46]
- janice 8/10/15 5:17 PM
Deleted: B4
- Cornell University 8/6/15 10:36 AM
Formatted [47]
- Cornell University 8/6/15 10:47 AM
Deleted: From observations, we have found a wide range in fractions of elements in individual site and all sites together, the ratio of the maximum and minimum in measured fractions could reach more than 700 for element K, and more than 200 for Ca and Mn. For the tuning ratio, we aim to bring the models closer to the observations at al... [48]
- janice 8/10/15 5:19 PM
Deleted: were ...re underestimated [49]
- ras486 8/9/15 3:27 PM
Deleted: e...crepancies may be beca... [50]
- janice 8/10/15 5:19 PM
Deleted: were
- ras486 8/9/15 3:28 PM
Deleted: e

metals in insoluble forms in dust particles could be from other sources such as the refractories and steel industries, construction, biomass burning or volcanic emissions (Castillo et al., 2008;Gaudichet et al., 1995; Hinkley et al., 1999; Paris et al., 2010).

The daily elemental fractions across all times and sites where there is data show that while the mean of the model was similar to the mean of the observations, there are some systematic differences (Figure 11a,b). The modeled elemental fractions are not as variable as the observations. This could be due to several issues. First there is a greater variability in the soil mineralogy and elemental composition of minerals than those included in the model (we only include the average values). Secondly, the dust model could introduce systematic errors (through advection, although this is likely to be small, as discussed in the methods section 2.1), or there could be some unaccounted anthropogenic particulate sources, modifying the dust aerosol. Also inconsistencies in the collection methods and differences in aerosol sampling periods and times, could yield the observed variations in elements as concluded by Lawrence and Neff (2009).

However, the ranges of the modeled fractions of P, Ca, Fe, K and Al are close to the dominant range of the observational fractions (Fig. 11a,b). The fractions of elements in dust measured are reported to be 0.5%-2.3% for Mg, 0.065-0.2% for P, 1.0-10.2% for Ca, 0.028%-0.124% for Mn, 1.3%-7.8% for Fe, 1.2%-4.6% for K, 3.7-12.7% for Al, and 22.4%-35.7% for Si (Wilke et al., 1984; Reheis and Kihl, 1995; Stoorvogel et al., 1997; Zhang et al., 1998; Yadav and Rajamani, 2004; Goudie and Middleton, 2006; Moreno et al., 2006; Jeong, 2008; Lawrence and Neff, 2009; Formenti et al., 2008; Desboeufs et al., 2010). The modeled elemental fraction in dust for P, Ca, Fe, K, Al and Si were similar to observations. However, the modeled fractions of Mg and Mn are lower (3.4 times and 3.5 times, respectively (Table 3)) than the observed ones for samples used in this study or of the above cited results. Underestimation of Mg and Mn could be due to a deficiency of minerals containing high concentrations of Mg and Mn in our model, as dolomite (MgCO₃) or palygorskyte ((Mg,Al)₂Si₄O₁₀(OH)·4(H₂O)) are often identified in dust particles for Mg (e.g. Diaz-Hernandes et al., 2011; Kalderon et al., 2009). Moreover, it is known that the chemical composition of minerals could be variable according to the regional origin of minerals and possible impurities. For example, the Mg content in calcite ranges from 0% to 2.7% in the natural environment (Titschack et al., 2011). But in this study, the assumed fraction of Mg in calcite is zero because we took calcite as a pure mineral (see Table 1). So the underestimation of Mg in dust could be a propagation of errors in previous compositions in minerals considered in this study.

Fig.10 Comparison of observed and modeled mean fractions of elements at each site for total suspended particulates (TSP). (1-Hetian, China; 2-Tazhong, China; 3-Yu Lin, China; 4-Duolun, China; 5-Shengsi, China; 6-Hanoi, Vietnam; 7-Marnila, Philippines; 8- Balad, Iraq; 9-Baghdad, Iraq; 10-Taji,Iraq; 11-Eilat; 12-Cape Verde Island; 13-Muswellbrook, Australia; 14-Richmond, Australia, 15-Tamanrasset, Algeria; 16-Banizoumbou, Niger; 17-Douz, Tunisia). Here we calculate the elemental fractions and average the fractions temporally for each site and compare to observations.

Cornell University 8/6/15 12:40 PM
Deleted: ed

janice 8/10/15 5:20 PM
Deleted: were

Cornell University 8/6/15 12:40 PM
Deleted: s

janice 8/10/15 5:20 PM
Deleted: we

Cornell University 8/6/15 10:47 AM
Deleted: .

ras486 8/9/15 3:30 PM
Deleted: ,

janice 8/10/15 5:20 PM
Deleted: were

ras486 8/9/15 3:30 PM
Deleted: and

janice 8/10/15 5:21 PM
Deleted: were

ras486 8/9/15 3:31 PM
Deleted: in

ras486 8/9/15 3:31 PM
Deleted:

janice 8/10/15 5:21 PM
Deleted: B4

yanzhang 8/2/15 3:02 PM
Formatted: Font color: Auto

Fig.11 Mean and quartile modeled and observational fractions of elements in (a) TSP and (b) PM_{2.5} for all sites together, the box line presents 25%, 50% and 75%, individually. Here we calculate the elemental fractions and average the fractions temporally for each site and compare to observations.

Table 3. Comparison of modeled and observed fractions of elements in TSP and tuning ratio based on 14-site measurements

For reference we show the comparison of the modeled dust deposition versus observed deposition (Fig. 12). The modeled dust deposition flux agrees well with observations. The correlation coefficient between modeled and observed dust deposition is 0.86. The median of model to observation ratio is 1.15. Overall the model has been tuned to represent dust deposition, concentration and Aerosol Optical Depth (AOD) (Albani, et al., 2014), however the model has difficulty matching both deposition and concentration observations, similar to other models (Huneus et al., 2011), suggesting more work on dust emission, transport and deposition processes is needed.

Fig.12 (a) Observational and (b) modeled dust deposition (g/m³/year). The scale is the same for both panels. (c) A scatter plot shows the comparison between the model and observations. The correlation coefficient between observations and model results reach 0.86.

3.5 Deposition of total and soluble dust elements over the ocean, land and ice sheets

Comparisons between observations and the model simulations presented here suggest some bias in the model results (Figure 11, Table 3); subsequently the model deposition values are adjusted to better match observed measurements by the tuning ratios (Table 3; Figure 13). Of course, improving our elemental estimates in the source region would be preferred in future studies. From the observations, we have found a wide range in fractions of elements at individual sites and at the sites together; the ratio of the maximum and minimum in measured fractions could reach more than 700 for element K, and more than 200 for Ca and Mn. Because of the limited observations, we use a global tuning factor, based on the median elemental %, and contrast this result with our default modeling approach (Table 3). It is noted that both the median of observed (3.10 %) and modeled (2.9 %) Fe was lower than 3.5%, which was thought to be the fraction of Fe in dust (e.g. Luo et al., 2008; Mahowald et al., 2008).

This study suggests significant variability in the elemental fractions in dust deposition (Figure 13, Table 4), and showed that the assumption that the fixed composition of dust being deposited over oceans is unlikely to be correct. Consistent with Mahowald et al. (2008), most dust deposition occurred downwind of dust generating regions bordering the North Atlantic, North Pacific and North Indian Ocean. The Greenland ice sheet accounted for the dominant part of elemental deposition to ice sheets regions, which is equal to the total amount of elements deposited in the whole of the South Atlantic Ocean. Fe and P are key elements in the marine ecosystem, with 6.3 Tg Fe and 184 Gg P added annually to all oceans and ice sheets (Table 5).

Table 4. Fractions (%) of elements in dust deposition into different ocean basins and ice sheets*

janice 8/7/15 9:02 PM
Formatted
yanzhang 8/2/15 2:59 PM
Deleted: B... 4
yanzhang 8/2/15 3:05 PM
Formatted
ras486 8/9/15 3:32 PM
Deleted:
janice 8/10/15 5:22 PM
Deleted: agreed
zhang yan 8/2/15 9:03 PM
Deleted: C
Cornell University 8/6/15 10:48 AM
Formatted
ras486 8/9/15 3:33 PM
Deleted: I and
yanzhang 8/2/15 3:05 PM
Deleted: B4
ras486 8/9/15 3:33 PM
Deleted: ,
janice 8/10/15 5:22 PM
Deleted: were
Cornell University 8/6/15 10:49 AM
Deleted: timing
yanzhang 8/2/15 3:06 PM
Deleted: B4
Cornell University 8/6/15 10:49 AM
Deleted:
Cornell University 8/6/15 12:42 PM
Formatted
ras486 8/9/15 3:34 PM
Deleted: in
Cornell University 8/6/15 12:42 PM
Formatted
ras486 8/9/15 3:36 PM
Deleted: either of...oth the median
Cornell University 8/6/15 12:42 PM
Formatted
zhang yan 8/2/15 9:02 PM
Deleted: For the tuning ratio, we air
Cornell University 8/6/15 12:42 PM
Deleted: s
yanzhang 8/2/15 3:14 PM
Deleted: 3..., and showed that the
ras486 8/9/15 3:39 PM
Deleted: receiving
yanzhang 8/2/15 3:15 PM
Deleted: e
ras486 8/9/15 3:39 PM
Deleted: ...emental deposited
yanzhang 8/2/15 3:15 PM
Deleted: ion
ras486 8/9/15 3:39 PM
Deleted: in
yanzhang 8/2/15 3:15 PM
Deleted: receiving an...hich is
ras486 8/9/15 3:38 PM
Deleted: summed
yanzhang 8/2/15 3:16 PM
ras486 8/9/15 3:40 PM
zhang yan 8/11/15 9:57 PM
zhang yan 8/2/15 8:45 PM

Also, the amounts of soluble dust element deposition are determined over different regions (see Section 2.1) (Figure 14). No atmospheric processing of natural dust or other sources of particles (e.g. anthropogenic sources) is included in this simulation. To better understand the uncertainties of soluble element deposition, estimates from two methods are used (Section 2.1) in simulating soluble elemental emission, transport and deposition. Fractional solubility of elements could not be estimated due to the lack of total element data from Method 2 (Sillanpaa (1982)). Spatial variations in fractional solubility of elements are identified by Sol-1 (mineral method) (Fig.14). Fractional solubility of Ca increases with distance from source regions because its solubility is higher in clay than in silt (Table 1b). Fractional solubility of modeled P in deposition ranges from 5% to 15%, with Saharan and Australian dust sources having solubilities averaging ~10%, consistent with Baker et al. (2006a;2006b). Previous observations suggest a fractional solubility for P of 7-100% [e.g., Graham and Duce, 1982; Chen et al., 1985; Bergametti et al., 1992; Herut et al., 1999, 2002; Ridame and Guieu, 2002]. Fractional solubility of Fe is 0.8%-1.2% in regions (Fig.14) where clay minerals such as illite play an important role (Journet et al., 2008) with a mean value of 1.17% of fractional Fe solubility (Table 1b). There is an obvious North-South gradient in the distribution of fractional solubility for Fe and Al, but with opposing magnitude (Fig.14). The fractional solubility could not be calculated using Sol-2 (Sillanpaa method) since total elemental fractions in soil were not reported in Sillanpaa (1982). Thus, the proportions of soluble Fe and K in total dust using two methods are compared with each other. This shows similar distribution patterns but the values are different (Fig. 15). The mineral method resulted in lower soluble Ca deposition and higher soluble Mg, P, Mn (Fig. 15). Our results suggest significant differences in the spatial distribution of solubility depending on which dataset is used to estimate soil solubility of elements. It should be noted that the solubility measurements by Sillanpaa (1982) were performed at different pH values (pH of 7 vs. 2) and media of extraction (acidified ultrapure waters vs. organic ligand solutions). It is known that pH and organic complexation greatly influence the fractional solubility, at least for Fe (e.g. Paris et al., 2011). Thus, that would explain the differences in elemental solubility that we computed for the dust. The soluble elemental deposition over ocean basins and ice sheets are determined using two methods and are listed in Table 5. Annual inputs of soluble Mg, P, Ca, Mn, Fe and K from mineral dust using method Sol-1 (Sol-2) were 0.28 (0.30) Tg, 16.89 (7.52) Gg, 1.32 (3.35) Tg, 22.84 (6.95) Gg, 0.068 (0.06) Tg, and 0.15 (0.25) Tg to oceans and ice sheets.

Fig.13 Percentages of elements in dust deposition (%) after tuning. It is tuned based on original percentages of elements in dust deposition in Fig. S1 by ratioing Obs./Mod. ratios listed in Table 3. Si did not change because there are not enough observational data available

Fig. 14 Fractional solubility of elements (soluble element / total element) in dust deposition (%):a. Mg, b. P, c. Ca, d. Mn, e. Fe, f. K, g. Al, h. Si

Fig. 15 Percentages of soluble elements in total dust deposition using (a) Sol-1 & (b) Sol-2 (%), Sol-1 refer to mineral method after tuning, Sol-2 refer to Sillanpaa method described in the methods section (2).

Table 4 Deposition of dust elements into different ocean basins and glaciers

- janice 8/10/15 5:24 PM
Formatted: Indent: First line: 0 cm
- janice 8/10/15 5:24 PM
Deleted: were ...re determined over ... [64]
- ras486 8/9/15 3:41 PM
Deleted: s
- janice 8/10/15 5:25 PM
Deleted: were
- ras486 8/9/15 3:41 PM
Deleted: i
- janice 8/10/15 5:25 PM
Deleted: Method ...ol-1 (mineral m ... [65]
- ras486 8/9/15 3:43 PM
Deleted: were...obvious North-Sout ... [66]
- janice 8/10/15 5:27 PM
Deleted: Method
- ras486 8/9/15 3:44 PM
Deleted: as...not reported in Silli ... [67]
- janice 8/10/15 5:29 PM
Deleted: were
- ras486 8/9/15 3:44 PM
Deleted: It...shows similar distribut ... [68]
- Cornell University 8/6/15 10:53 AM
Deleted: vs...s. 2) and media of extr ... [69]
- ras486 8/9/15 3:45 PM
Deleted: s...solutions). It is known ... [70]
- janice 8/10/15 5:29 PM
Deleted: were
- zhang yan 8/11/15 9:57 PM
Deleted: 4
- janice 8/10/15 5:30 PM
Deleted: M1 ...ol-1 (M2 ... [71]
- yanzhang 8/2/15 3:16 PM
Deleted: Tuned ...percentages of el ... [72]
- yanzhang 8/2/15 3:17 PM
Deleted: M... & (b) Sol-M... (%), ... [73]

4 Summary and Conclusions

A new technique combining soil and mineralogical datasets is introduced to estimate the global emission inventory of soil associated elements Mg, P, Ca, Mn, Fe, K, Al, and Si. The spatial elemental dust emissions, transport and deposition are simulated using CESM from 2001-2010. Spatial variability of soil element fractions is characterized globally (Fig 2), and shows that the use of a constant element fraction in dust across the globe is not consistent with existing observational data for Ca and Al (Fig 10 and 11). There are few observations for elemental distributions in source regions to verify these emission, concentration and deposition simulations, but for some elements (Ca and Al), the soil elemental distribution combined with the transported dust flux in the model better captures the percentage of chemical elements in dust concentrations observed (Figure 10, 11). However, both Mg and Mn levels are underestimated by the model using the present mineral maps. The correlation of the percent of elements is not statistically significant for several elements (Mg, Mn, P and K), suggesting that improvements in the soil inventories or simulations is required, although these results could also be due to low numbers of observations. The observations and model results suggest the elemental fractions in dust varied globally and between different dust production regions, especially for Ca with values from 1% to 30%. The ratio of Ca/Al, ranged between 0.1-5.0, and is confirmed as an indicator of dust source regions (Zhang et al., 1997; Zhang et al., 2003; Sun et al., 2004a,b; Shen et al., 2007). For Fe in TSP, the median of modeled fraction is 2.90%, less than the commonly assumed 3.5% Fe used in dust models (e.g. Luo et al., 2008; Mahowald et al., 2008).

Seasonal variability of emission, concentration and deposition of most elements are simulated in the model. Also, different soluble elemental datasets show that the fractional solubility of elements varies spatially. Mineral dust element deposition fluxes into ocean basins are updated using a variable fractional elemental inventory and could have potentially important impacts on evaluating their biogeochemical effects. This study shows that soil emission inventories do a fairly good job at predicting dust elemental concentrations during dust events, except for Mg and Mn. However, the high spatial heterogeneity in elemental distributions is not captured in the model. Several sources of uncertainties exist in the model projections, the largest of which is likely to be the assumptions in the soil mappings from soil types to minerals to elemental distributions. In the future, these dust emission inventories can be combined with anthropogenic elemental inventories to further improve our understanding of elemental deposition to the oceans.

Acknowledgements

We would like to thank the US Department of Defense (DOD) for sharing chemical data from their Enhanced Particulate Matter Surveillance Program (EPMS), and anonymous reviewers for helpful comments. We acknowledge the support of NSF grant 0932946 and 1137716 and DOE-SC0006735. Simulations were conducted on the NSF National Center for Atmospheric Research's supercomputers.

- janice 8/10/15 5:30 PM
Deleted: was
- janice 8/10/15 5:30 PM
Deleted: were
- janice 8/10/15 5:30 PM
Deleted: was
- janice 8/10/15 5:31 PM
Deleted: showed
- janice 8/10/15 5:31 PM
Deleted: captured
- ras486 8/9/15 3:47 PM
Deleted: and
- janice 8/10/15 5:31 PM
Deleted: were
- janice 8/10/15 5:31 PM
Deleted: was
- janice 8/10/15 5:32 PM
Deleted:
- ras486 8/9/15 3:49 PM
Deleted: highest values of 30% and lowest of 1%.
- janice 8/10/15 5:32 PM
Deleted: was
- ras486 8/9/15 3:51 PM
Deleted: , a flat value usually used in dust model study
- ras486 8/9/15 3:51 PM
Deleted: s
- ras486 8/9/15 3:51 PM
Deleted: and thus
- janice 8/10/15 5:32 PM
Deleted: were
- janice 8/10/15 5:32 PM
Deleted: ed
- janice 8/10/15 5:32 PM
Deleted: varied
- ras486 8/9/15 3:51 PM
Deleted: s
- janice 8/10/15 5:33 PM
Deleted: were
- Cornell University 8/6/15 9:55 AM
Deleted: T
- janice 8/10/15 5:33 PM
Deleted: was
- yanzhang 8/2/15 6:26 PM
Deleted: US funding
- yanzhang 8/2/15 6:27 PM
Deleted: from

Reference

- [Albani, S., Mahowald, N. M., Perry, A. T., Scanza, R. A., Zender, C. S., Heavens, N. G., Maggi, V., Kok, J. F., and Otto-Bliesner, B. L.: Improved dust representation in the Community Atmosphere Model, *J. Adv. Model. Earth Syst.*, 6, 541–570, doi:10.1002/2013MS000279, 2014.](#)
- [Astitha, M., Lelieveld, J., Abdel Kader, M., Pozzer, A., and de Meij, A.: Parameterization of dust emissions in the global atmospheric chemistry-climate model EMAC: impact of nudging and soil properties, *Atmos. Chem. Phys.*, 12, 11057–11083, doi:10.5194/acp-12-11057-2012, 2012.](#)
- [Baker, A. R., Kelly, S. D., Biswas, K. F., Witt, M., and Jickells, T. D.: Atmospheric deposition of nutrients to the Atlantic Ocean, *Geophys. Res. Lett.*, 30, 2296, doi:10.1029/2003GL018518, 2003.](#)
- [Baker, A. R., French, M., and Linge, K. L.: Trends in aerosol nutrient solubility along a west–east transect of the Saharan dust plume, *Geophys. Res. Lett.*, 33, L07805, doi:10.1029/2005GL024764, 2006a.](#)
- [Baker, A. R., Jickells, T. D., Witt, M., and Linge, K. L.: Trends in the solubility of iron, aluminum, manganese and phosphorus collected over the Atlantic Ocean, *Mar. Chem.*, 98, 43–58, doi:10.1016/j.marchem.2005.06.004, 2006b.](#)
- [Baker, A. R. and Croot, P. L.: Atmospheric and marine controls on aerosol iron solubility in seawater, *Mar. Chem.*, 120, 4–13, 2010.](#)
- [Bergametti, G., Gomes, L., Coudé-Gaussen, G., Rognon, P. and Le Coustumer, M.: African dust observed over Canary Islands: Source-regions identification and transport pattern for some summer situations, *J. Geophys. Res.*, 12, 14855–14864, doi:10.1029/JD094iD12p14855, 1989.](#)
- [Bergametti, G., Remoudaki, E., Losno, R., Steiner, E., Chatenet, B., and Buat-Menard, P.: Source, transport and deposition of atmospheric phosphorus over the northwestern Mediterranean, *J. Atmos. Chem.*, 14, 501–513, doi:10.1007/BF00115254, 1992.](#)
- [Boyd, P., Wong, C., Merrill, J., Whitney, F., Snow, J., Harrison, P., and Gower, J.: Atmospheric iron supply and enhanced vertical carbon flux in the NE subsarctic Pacific: is there a connection? *Global Biogeochem. Cy.*, 12, 429–441, 1998.](#)
- [Buck, C., Landing, W. M., Resing, J. A., and Lebon, G.: Aerosol iron and aluminum solubility in the northwest Pacific Ocean: results from the 2002 IOC Cruise, *Geochem. Geophys. Geosy.*, 7, Q04M07, doi:10.1029/2005GC000977, 2006.](#)
- [Capone, D. G., Zehr, J. P., Paerl, H. W., Bergman, B., and Carpenter, E. J.: Trichodesmium, a globally significant marine cyanobacterium, *Science*, 276, 1221–1229, 1997.](#)
- [Carpenter, L. J., Fleming, Z. L., Read, K. A., Lee, J. D., Moller, S. J., Hopkins, J. R., Purvis, R. M., Lewis, A. C., Müller, K., Heinold, B., Herrmann, H., Fomba, K. W., Pinxteren, D. v., Müller, C., Tegen, I., Wiedensohler, A., Müller, T., N. Niedermeier, Achterberg, E. P., Patey, M. D., Kozlova, E. A., Heimann, M., Heard, D. E., Plane, J. M. C., Mahajan, A., Oetjen, H., Ingham, T., Stone, D., Whalley, L. K., Evans, M. J., Pilling, M. J., Leigh, R. J., Monks, P. S., Karunaharan, A., Vaughan, S., Arnold, S. R., Tschirmer, J., Pöhler, D., Frieß, U., Holla, R., Mendes, L. M., Lopez, H., Faria, B., Manning, A. J., and Wallace, D. W. R.: Seasonal characteristics of tropical marine boundary layer air measured at the Cape Verde Atmospheric Observatory, *J. Atmos. Chem.*, 67, 87–140, doi:10.1007/s10874-011-9206-1, 2010.](#)
- [Castillo, S., Moreno, T., Querol, X., Alastuey, A., Cuevas, E., Herrmann, L., Monkaila, M., and Gibbons, W.: Trace element variation in size-fractionated African desert dusts, *J. Arid Environ.* 72, 1034–1045, 2008.](#)
- [Chen, L., Arimoto, R., and Duce, R. A.: The sources and forms of phosphorus in marine aerosol particles and rain from Northern New Zealand, *Atmos. Environ.*, 19, 779–787, 1985.](#)

[Chen, H.-Y., Fang, T.-H., Preston, M., and Lin, S.: Characterization of phosphorus in the aerosol of a coastal atmosphere: using an sequential extraction method, Atmos. Environ., 40, 279–289, doi:10.1016/j.atmosenv.2005.09.051, 2006.](#)

[Chen, Y. and Siefert, R.: Sesaonal and spatial distributions and dry deposition fluxes of atmospheric total and labile iron over the tropical and subtropical North Atlantic Ocean, J. Geophys. Res., 109, D09305, doi:10.1029/2003JD003958, 2004.](#)

[Chen, Y., Paytan, A., Chase, Z., Measures, C., Beck, A. J., Sañudo-Wilhelmy, S. A., and Post, A. F.: Sources and fluxes of atmospheric trace elements to the Gulf of Aqaba, Red Sea, J. Geophys. Res., 113, D05306, doi:10.1029/2007JD009110, 2008.](#)

[Claquin, T., Schulz, M., and Balkanski, Y. J.: Modeling the mineralogy of atmospheric dust sources, J. Geophys. Res., 104, 22243–22256, 1999.](#)

[Cohen, D. D., Stelcer, E., Hawas, O., and Garton, D.: IBA methods for characterisation of fine particulate atmospheric pollution: a local, regional and global research problem, Nucl. Instrum. Meth. B, 219, 145–152, 2004.](#)

[Cohen, D. D., Stelcer, E., Garton, D., and Crawford, J.: Fine particle characterization, source apportionment and long range dust transport into the Sydney Basin: a long term study between](#)

[1998 and 2009, Atmospheric Pollution Research, 2, 182–189, 2011.](#)

[Desboeufs, K., Journet, E., Rajot, J.-L., Chevaillier, S., Triquet, S., Formenti, P., and Zakou, A.: Chemistry of rain events in West Africa: evidence of dust and biogenic influence in convective systems, Atmos. Chem. Phys., 10, 9283–9293, doi:10.5194/acp-10-9283-2010, 2010.](#)

[Duce, R. A. and Tindale, N. W.: Atmospheric transport of iron and its deposition in the ocean, Limnol. Oceanogr., 36, 1715–1726, 1991.](#)

[Christian, J.R. Advection in plankton models with variable elemental ratios. Ocean Dynamics, 57\(1\), 63-71, doi:10.1007/s10236-006-0097-7, 2007.](#)

[Duce, R. A., Liss, P. S., Merrill, J. T., Atlas, E. L., Buat-Meard, P., Hicks, B. B., Miller, J. M., Prospero, J. M., Arimoto, R., Church, T. M., Ellis, W., Galloway, J. N., Hansen, L., Jickels, T. D., Knap, A. H., Reinhardt, K. H., Schneider, B., Soudine, A., Tokos, J. J., Tsunogai, S., Wollast, R., and Zhou, M.: The atmospheric input of trace species to the world ocean, Global Biogeochem. Cy., 5, 193–259, 1991.](#)

[Engelbrecht, J., McDonald, E., Gillies, J., Jayanty, R. K. M., Casuccio, G., and Gertler, A. W.: Characterizing mineral dusts and other aerosols from the Middle East – Part 1: Ambient sampling, Inhal. Toxicol., 21, 297–326, 2009.](#)

[Engelbrecht, J. P., Menendez, I., and Derbyshire, E.: Sources of PM_{2.5} impacting on Gran Canaria, Spain, Catena, 117, 119–132, doi:10.1016/j.catena.2013.06.017, 2014.](#)

[FAO-Unesco: Soil Map of the World, Southeast Asia, 1976, Sheet IX, Edition I, 1976.](#)

[Formenti, P., Rajot, J. L., Desboeufs, K., Caquineau, S., Chevaillier, S., Nava, S., Gaudichet, A., Journet, E., Triquet, S., Alfaro, S., Chiari, M., Haywood, J., Coe, H., and Highwood, E.: Regional variability of the composition of mineral dust from western Africa: results from the AMMA SOP0/DABEX and DODO field campaigns, J. Geophys. Res., 113, D00C13,](#)

[doi:10.1029/2008JD009903, 2008.](#)

[Formenti, P., Schütz, L., Balkanski, Y., Desboeufs, K., Ebert, M., Kandler, K., Petzold, A., Scheuven, D., Weinbruch, S., and Zhang, D.: Recent progress in understanding physical and chemical properties of African and Asian mineral dust, Atmos. Chem. Phys., 11, 8231–8256, doi:10.5194/acp-11-8231-2011, 2011.](#)

janice 8/7/15 6:42 PM
Formatted: Font:(Default) Times New Roman, 10 pt

zhang yan 8/8/15 12:39 AM
Deleted: - ... [74]

janice 8/7/15 6:42 PM
Formatted: Font:(Default) Times New Roman, 10 pt

[Fung, I., Meyn, S. K., Tegen, I., Doney, S., John, J., and Bishop, J.: Iron supply and demand in the upper ocean, *Global Biogeochem. Cy.*, 14, 281–295, 2000.](#)

[Gaudichet, A., Echalar, F., Chatenet, B., Quisefit, J. P., Malingre, G., Cachier, H., Buatmenard, P., Artaxo, P., and Maenhaut, W.: Trace elements in tropical African savanna biomass burning aerosols, *J. Atmos. Chem.*, 22, 19–39, 1995.](#)

[Gold, C. M., Cavell, P. A., and Smith, D. G. W.: Clay minerals in mixtures: sample preparation, analysis, and statistical interpretation, *Clay. Clay Miner.*, 3, 191–199, 1983.](#)

[Goudie, A. S. and Middleton, N. J.: *Desert Dust in the Global System*, Springer, Berlin, 2006.](#)

[Graham, W. F. and Duce, R. A.: The atmospheric transport of phosphorus to the western North Atlantic, *Atmos. Environ.*, 16, 1089–1097, doi:10.1016/0004-6981\(82\)90198-6, 1982.](#)

[Guieu, C., Bonnet, S., Wagener, T., and Loye-Pilot, M.-D.: Biomass burning as a source of dissolved iron to the open ocean?, *Geophys. Res. Lett.*, 22, L19608, doi:10.1029/2005GL022962, 2005.](#)

[Guo, L., Chen, Y., Wang, F. J., Meng, X., Xu, Z. F., and Zhuang, G.: Effects of Asian dust on the atmospheric input of trace elements to the East China Sea, *Mar. Chem.*, 163, 19–27, doi:10.1016/j.marchem.2014.04.003, 2014.](#)

[Hand, J. L., Mahowald, N. M., Chen, Y., Siefert, R. L., Luo, C., Subramaniam, A., and Fung, I.: Estimates of atmospheric-processed soluble iron from observations and a global mineral aerosol model: Biogeochemical implications, *J. Geophys. Res.*, 109, D17205, doi:10.1029/2004JD004574, 2004.](#)

[Herut, B., Krom, M., Pan, G., and Mortimer, R.: Atmospheric input of nitrogen and phosphorus to the southeast Mediterranean: sources, fluxes and possible impact, *Limnol. Oceanogr.*, 44, 1683–1692, 1999.](#)

[Herut, B., Collier, R., and Krom, M.: The role of dust in supplying nitrogen and phosphorus to the southeast Mediterranean, *Limnol. Oceanogr.*, 47, 870–878, 2002.](#)

[Herut, B., Zohary, T., Krom, M. D., Mantoura, R. F. C., Pitta, V., Psarra, S., Rassoulzadegan, F., Tanaka, T., and Thingstad, F. T.: Response of east Mediterranean surface water to Saharan dust: on-board microcosm experiment and field observations, *Deep-Sea Res. Pt. II*, 52, 3024–3040, doi:10.1016/j.dsr2.2005.09.003, 2005.](#)

[Hinkley, T. K., Lamothe, P. J., Wilson, S. A., Finnegan, D. L., and Gerlach, T. M.: Metal emissions from Kilauea, and a suggested revision of the estimated worldwide metal output by quiescent degassing of volcanoes, *Earth Planet. Sc. Lett.*, 170, 315–325, 1999.](#)

[Huneeus, N., Schulz, M., Balkanski, Y., Griesfeller, J., Prospero, J., Kinne, S., Bauer, S., Boucher, O., Chin, M., Dentener, F., Diehl, T., Easter, R., Fillmore, D., Ghan, S., Ginoux, P., Grini, A., Horowitz, L., Koch, D., Krol, M. C., Landing, W., Liu, X., Mahowald, N., Miller, R., Morcrette, J.-J., Myhre, G., Penner, J., Perlwitz, J., Stier, P., Takemura, T., and Zender, C. S.: Global dust model intercomparison in AeroCom phase I, *Atmos. Chem. Phys.*, 11, 7781–7816, doi:10.5194/acp-11-7781-2011, 2011.](#)

[Jeong, G. Y.: Bulk and single-particle mineralogy of Asian dust and a comparison with its source soils, *J. Geophys. Res.*, 113, D02208, doi:10.1029/2007jd008606, 2008.](#)

[Jickells, T., An, Z., Andersen, K., Baker, A., Bergametti, G., Brooks, N., Cao, J., Boyd, P., Duce, R., Hunter, K., Kawahata, H., Kubilay, N., LaRoche, J., Liss, P., Mahowald, N., Prospero, J., Ridgwell, A., Tegen, I., and Torres, R.: Global iron connections between dust, ocean biogeochemistry and climate, *Science*, 308, 67–71, 2005.](#)

[Journet, E., Desboeufs, K. V., Caquineau, S., and Colin, J.-L.: Mineralogy as a critical factor of dust iron solubility, *Geophys. Res. Lett.*, 35, L07805, doi:10.1029/2007gl031589, 2008.](#)

[Journet, E., Balkanski, Y., and Harrison, S. P.: A new data set of soil mineralogy for dust-cycle modeling, *Atmos. Chem. Phys.*, 14, 3801–3816, doi:10.5194/acp-14-3801-2014, 2014.](#)

[Kandler, K., Benker, N., Bundke, U., Cuevas, E., Ebert, M., Knippertz, P., Rodríguez, S., Schütz, L., and Weinbruch, S.: Chemical composition and complex refractive index of Saharan mineral dust at Izaña, Tenerife \(Spain\) derived by electron microscopy, *Atmos. Environ.*, 41, 8058–8074, 2007.](#)

[Kok, J. F.: A scaling theory for the size distribution of emitted dust aerosols suggests climate models underestimate the size of the global dust cycle, *P. Natl. Acad. Sci. USA*, 108, 1016–021, 2011.](#)

[Kreutz, K. J. and Sholkovitz, E. R.: Major element, rare earth element, and sulfur isotopic composition of a high-elevation firn core: sources and transport of mineral dust in central Asia, *Geochem. Geophys. Geosy.*, 1, 1048–1071, 2000.](#)

[Lam, P. and Bishop, J.: The continental margin is a key source of iron to the North Pacific Ocean, *Geophys. Res. Lett.*, 35, L07608, doi:10.1029/2008GL033294, 2008.](#)

[Lawrence, C. R. and Ne, J. C.: The physical and chemical flux of eolian dust across the landscape: a synthesis of observations and an evaluation of spatial patterns, *Chem. Geol.*, 267, 46–63, doi:10.1016/j.chemgeo.2009.02.005, 2009.](#)

[Li, G., Chen, J., Chen, Y., Yang, J., Ji, J., and Liu, L.: Dolomite as a tracer for the source regions of Asian dust, *J. Geophys. Res.*, 112, D17201, doi:10.1029/2007jd008676, 2007.](#)

[Lin, S.-J., and R. B. Rood. An explicit flux-form semi-Lagrangian shallow-water model on the sphere, *Quarterly Journal of the Royal Meteorological Society*, 123, 2477–2498, 1997.](#)

[Luo, C., Mahowald, N., Bond, T., Chuang, P. Y., Artaxo, P., Siefert, R., Chen, Y., and Schauer, J.: Combustion iron distribution and deposition, *Global Biogeochem. Cy.*, 22, GB1012, doi:10.1029/2007GB002964, 2008.](#)

[Mahowald, N.; Baker, A.; Bergametti, G.; Brooks, N.; Duce, R.; Jickells, T.; Kubilay, N.; Prospero, J.; Tegen, I. Atmospheric global dust cycle and iron inputs to the ocean, *Global Biogeochem. Cy.*, 19, GB4025, doi:10.1029/2004GB002402, 2005.](#)

[Mahowald, N., Muhs, D. R., Levis, S., Rasch, P. J., Yoshioka, M., Zender, C. S., and Luo, C.: Change in atmospheric mineral aerosols in response to climate: last glacial period, preindustrial, modern, and doubled carbon dioxide climates, *J. Geophys. Res.-Atmos.*, 111, D10202, doi:10.1029/2005JD006653, 2006.](#)

[Mahowald, N., Jickells, T. D., Baker, A. R., Artaxo, P., Benitez-Nelson, C. R., Bergametti, G., Bond, T. C., Chen, Y., Cohen, D. D., Herut, B., Kubilay, N., Losno, R., Luo, C., Maenhaut, W., McGee, K. A., Okin, G. S., Siefert, R. L., and Tsukuda, S.: Global distribution of atmospheric phosphorus sources, concentrations and deposition rates, and anthropogenic impacts, *Global Biogeochem. Cy.*, 22, GB4026, doi:10.1029/2008GB003240, 2008.](#)

[Marino, F., Maggi, V., Delmonte, B., Ghermandi, G., and Petit, J. R.: Elemental composition \(Si, Fe, Ti\) of atmospheric dust over the last 220 kyr from the EPICA ice core \(Dome C, Antarctica\), *Ann. Glaciol.*, 39, 110–118, doi:10.3189/172756404781813862, 2004.](#)

[Marteel, A., Gaspari, V., Boutron, C. F., Barbante, C., Gabrielli, P., Cescon, P., Ferrari, C., Dommergue, A., Rosman, K., Hong, S., and Hur, S.: Climate-related variations in crustal trace elements in Dome C \(East Antarctica\) ice during the past 672 kyr, *Climatic Change*, 92, 191–211, 2009.](#)

[Martin, J. H., Gordon, R. M., and Fitzwater, S. E.: The case for iron, *Limnol. Oceanogr.*, 36, 1793–1802, 1991.](#)

[Measures, C. and Vink, S.: On the use of dissolved aluminum in surface waters to estimate dust deposition to the ocean, *Global Biogeochem. Cy.*, 14, 317–327, 2000.](#)

[Mermut, A. R. and Cano, A. F.: Baseline studies of the clay minerals society source clays: chemical analyses of major elements, *Clay. Clay Miner.*, 49, 381–386, 2001.](#)

[Mills, M. M., Ridame, C., Davey, M., LaRoche, J., and Geider, R.: Iron and phosphorus co-limit nitrogen fixation in](#)

zhang yan 8/8/15 12:38 AM
Formatted: Font:(Default) Times New Roman, 10 pt, Font color: Auto, (Asian) Chinese (PRC)

zhang yan 8/8/15 12:38 AM
Formatted: Justified, Space After: 0.5 line, Line spacing: multiple 1.15 li

zhang yan 8/8/15 12:38 AM
Formatted: Font:(Default) Times New Roman, 10 pt, (Asian) Chinese (PRC)

[the eastern tropical North Atlantic, *Nature*, 429, 292–294, 2004.](#)

[Moore, J. K. and Braucher, O.: Sedimentary and mineral dust sources of dissolved iron to the world ocean, *Biogeosciences*, 5, 631–656, doi:10.5194/bg-5-631-2008, 2008.](#)

[Morel, F. M. M., Milligan, A. J., and Saito, M. A.: Marine bioinorganic chemistry: the role of trace metals in the oceanic cycles of major nutrients, in: *Treatise on Geochemistry*, Vol. 6., Elsevier, Pergamon, Oxford, 113–143, ISBN 0-08-043751-6, 2003.](#)

[Moreno, T., Querol, X., Castillo, S., Alastuey, A., Cuevas, E., Herrmann, L., Mounkaila, M., Elvira, J., and Gibbons, W.: Geochemical variations in aeolian mineral particles from the Sahara-Sahel dust corridor, *Chemosphere*, 65, 261–270, 2006.](#)

[Nickovic, S., Vukovic, A., Vujadinovic, M., Djurdjevic, V., and Pejanovic, G.: Technical Note: High-resolution mineralogical database of dust-productive soils for atmospheric dust modeling, *Atmos. Chem. Phys.*, 12, 845–855, doi:10.5194/acp-12-845-2012, 2012.](#)

[Nickovic S., Vukovic A., Vujadinovic M. \(2013\). Atmospheric processing of iron carried by mineral dust, *Atmos. Chem. Phys.*, 13, 9169–9181, doi:10.5194/acp-13-9169-2013, 2013.](#)

[Nozaki, Y.: A fresh look at element distribution in the North Pacific, *EOS T. Am. Geophys. Un.*, 78, 221–221, doi:10.1029/97EO00148, 1997.](#)

[Okin, G. S., Mahowald, N., Chadwick, O. A., and Artaxo, P.: Impact of desert dust on the biogeochemistry of phosphorus in terrestrial eco-systems, *Global Biogeochem. Cy.*, 18, GB2005, doi:10.1029/2003GB002145, 2004.](#)

[Paris, R., Desboeufs, K. V., Formenti, P., Nava, S., and Chou, C.: Chemical characterization of iron in dust and biomass burning aerosols during AMMA-SOP0/DABEX: implication for iron solubility, *Atmos. Chem. Phys.*, 10, 4273–4282, doi:10.5194/acp-10-4273-2010, 2010.](#)

[Paytan, A., Mackey, K., Chen, Y., Lima, I., Doney, S., Mahowald, N., Lablosa, R., and Post, A.: Toxicity of atmospheric aerosols on marine phytoplankton, *P. Natl. Acad. Sci. USA*, 106, 106, 4601–4605, doi:10.1073/pnas.0811486106, 2009.](#)

[Perry, K. D., Cahill, T. A., Eldred, R. A., Dutcher, D. D., and Gill, T. E.: Long-range transport of North African dust to the eastern United States, *J. Geophys. Res.-Atmos.*, 102, 11225–11238, 1997.](#)

[Petrucci, R. H., Harwood, W. S., Herring, G., Madura, J.: *General Chemistry: Principles and Modern Application*, 9th edn., Prentice Hall, New Jersey, Pearson2001.](#)

[Prospero, J. M., Landing, W. M., and Schulz, M.: African dust deposition to Florida: temporal and spatial variability and comparisons to models, *J. Geophys. Res.*, 115, D13304, doi:10.1029/2009JD012773, 2010.](#)

[Rasch, P., D. Coleman, N. Mahowald, D. Williamson, S.-J. Lin, B. Boville, and P. Hess. Characteristics of atmospheric transport using three numerical formulations for atmospheric dynamics in a single GCM framework, *Journal of Climate*, 19, 2243–2266, 2006.](#)

[Reheis, M. C. and Kihl, R.: Dust deposition in southern Nevada and California, 1984–1989 –relations to climate, source area, and source lithology, *J. Geophys. Res.-Atmos.*, 100, 8893–8918, 1995.](#)

[Reid, E. A., Reid, J. S., Meier, M. M., Dunlap, M. R., Collins, S. S., Broumas, A., Perry, K., and Maring, H.: Characterization of African dust transported to Puerto Rico by individual particle and size segregated bulk analysis, *J. Geophys. Res.*, 108, 8591, doi:10.1029/2002JD002935, 2003.](#)

[Ridame, C. and Guieu, C.: Saharan input of phosphate to the oligotrophic water of the open western Mediterranean](#)

zhang yan 8/2/15 9:14 PM

Formatted: Indent: Left: 0 cm, Hanging: 3.6 ch, Widow/Orphan control, Adjust space between Latin and Asian text, Adjust space between Asian text and numbers

zhang yan 8/8/15 12:38 AM

Formatted: Font:(Default) Times New Roman, 10 pt, Font color: Auto, (Asian) Chinese (PRC)

[Sea, Limnol. Oceanogr., 47, 856–869, 2002.](#)

[Scanza, R. A., Mahowald, N., Ghan, S., Zender, C. S., Kok, J. F., Liu, X., and Zhang, Y.: Modeling dust as component minerals in the Community Atmosphere Model: development of framework and impact on radiative forcing, Atmos. Chem. Phys., 15, 537–561, 2015.](#)

[Schütz, L. and Rahn, K. A.: Trace element concentrations in erodible soils, Atmos. Environ., 16, 171–176, 1982.](#)

[Seinfeld, J. H. and Pandis, S. N.: Atmospheric Chemistry and Physics: from Air Pollution to Climate Change, J. Wiley, New York, 1998.](#)

[Shao, Y.: A model for mineral dust emission, J. Geophys. Res., 106, 20239–20254, doi:10.1029/2001jd900171, 2001.](#)

[Shen, Z. X., Li, X., Cao, J., Caquineau, S., Wang, Y., and Zhang, X.: Characteristics of clay minerals in Asian dust and their environmental significance, China Part., 3, 260–264, 2005.](#)

[Shen, Z. X., Cao, J., Li, X., Okuda, T., Wang, Y., and Zhang, X.: Mass concentration and mineralogical characteristics of aerosol particles collected at Dunhuang during ACE-Asia, Adv. Atmos. Sci., 23, 291–298, 2006.](#)

[Shen, Z. X., Cao, J. J., Arimoto, R., Zhang, R. J., Jie, D. M., Liu, S. X., Zhu, C. S.: Chemical composition and source characterization of spring aerosol over Horqin sand land in northeastern China, J. Geophys. Res., 112, D14315, doi:10.1029/2006JD007991, 2007.](#)

[Sillanpää, M.: Micronutrients and the Nutrient Status of Soils: a Global Study, FAO Soils Bulletin, No. 48., Appendix 6–7, Rome, 1982.](#)

[Stoorvogel, J. J., VanBreemen, N., and Janssen, B. H.: The nutrient input by Harmattan dust to a forest ecosystem in Côte d'Ivoire, Africa, Biogeochemistry, 37, 145–157, 1997.](#)

[Sun, Y., Zhuang, G., Yuan, H., Zhang, X., and Guo, J.: Characteristics and sources of 2002 super dust storm in Beijing, Chinese Sci. Bull., 49, 698–705, 2004a.](#)

[Sun, Y., Zhuang, G., Wang, Y., Han, L., Guo, J., Dan, M., Zhang, W., Wang, Z., and Hao, Z.: The air-borne particulate pollution in Beijing – concentration, composition, distribution and sources, Atmos. Environ., 38, 5991–6004, 2004b.](#)

[Svensson, A., Biscaye, P. E., and Grousset, F. E.: Characterization of late glacial continental dust in the Greenland Ice Core Project ice core, J. Geophys. Res., 105, 4637–4656, doi:10.1029/1999jd901093, 2000.](#)

[Swap, R., Garstang, M., Greco, S., Talbot, R., and Kallberg, P.: Saharan dust in the Amazon Basin, Tellus B, 44, 133–149, 1992.](#)

[Textor, C., Schulz, M., Guibert, S., Kinne, S., Balkanski, Y., Bauer, S., Bernsten, T., Berglen, T., Boucher, O., Chin, M., Dentener, F., Diehl, T., Easter, R., Feichter, H., Fillmore, D., Ghan, S., Ginoux, P., Gong, S., Grini, A., Hendricks, J., Horowitz, L., Huang, P., Isaksen, I., Iversen, I., Kloster, S., Koch, D., Kirkevåg, A., Kristjansson, J. E., Krol, M., Lauer, A., Lamarque, J. F., Liu, X., Montanaro, V., Myhre, G., Penner, J., Pitari, G., Reddy, S., Seland, Ø., Stier, P., Takemura, T., and Tie, X.: Analysis and quantification of the diversities of aerosol life cycles within AeroCom, Atmos. Chem. Phys., 6, 1777–1813, doi:10.5194/acp-6-1777-2006, 2006.](#)

[Textor, C., Schulz, M., Guibert, S., Kinne, S., Balkanski, Y., Bauer, S., Bernsten, T., Berglen, T., Boucher, O., Chin, M., Dentener, F., Diehl, T., Feichter, J., Fillmore, D., Ginoux, P., Gong, S., Grini, A., Hendricks, J., Horowitz, L., Huang, P., Isaksen, I. S. A., Iversen, T., Kloster, S., Koch, D., Kirkevåg, A., Kristjansson, J. E., Krol, M., Lauer, A., Lamarque, J. F., Liu, X., Montanaro, V., Myhre, G., Penner, J. E., Pitari, G., Reddy, M. S., Seland, Ø., Stier, P., Takemura, T., and Tie, X.: The effect of harmonized emissions on aerosol properties in global models – an AeroCom experiment, Atmos. Chem. Phys., 7, 4489–4501, doi:10.5194/acp-7-4489-2007, 2007.](#)

zhang yan 8/2/15 9:16 PM

Formatted: Font:(Default) Times New Roman, 10 pt, Font color: Auto, (Asian) Chinese (PRC)

[Titschack, J., Goetz-Neunhoefer, F., and Neubauer, J.: Magnesium quantification in calcites \[\(Ca,Mg\)CO₃\] by Rietveld-based XRD analysis: revisiting a well-established method, *Am. Mineral.*, 96, 1028–1038, 2011.](#)

[Wang, Q., Zhuang, G., Li, J., Huang, K., Zhang, R., Jiang, Y., Lin, Y., and Fu, J. S.: Mixing of dust with pollution on the transport path of Asian dust – revealed from the aerosol over Yulin, the north edge of Loess Plateau, *Sci. Total Environ.*, 409, 573–581, 2010.](#)

[Werner, M., Tegen, I., Harrison, S. P., Kohfeld, K. E., Prentice, I. C., Balkanski, Y., Rodhe, H., and Roelandt, C.: Seasonal and interannual variability of the mineral dust cycle under present and glacial climate conditions, *J. Geophys. Res.*, 107, D244744, doi:10.1029/2002JD002365, 2002.](#)

[Wilke, B. M., Duke, B. J., and Jimoh, W. L. O.: Mineralogy and chemistry of Harmattan dust in northern Nigeria, *Catena*, 11, 91–96, 1984.](#)

[Xuan, J., Sokolik, I. N., Hao, J., Guo, F., Mao, H., and Yang, G.: Identification and characterization of sources of atmospheric mineral dust in East Asia, *Atmos. Environ.*, 38, 6239–6252, 2004.](#)

[Yadav, S. and Rajamani, V.: Geochemistry of aerosols of northwestern part of India adjoining the Thar Desert, *Geochim. Cosmochim. Ac.*, 68, 1975–1988, 2004.](#)

[Zender, C., Bian, H., and Newman, D.: Mineral Dust Entrainment and Deposition \(DEAD\) model: description and 1990s dust climatology, *J. Geophys. Res.*, 108, 4416, doi:10.1029/2002JD002775, 2003.](#)

[Zhang, X. Y., Arimoto, R., and An, Z. S.: Dust emission from Chinese desert sources linked to variation in atmospheric circulation, *J. Geophys. Res.*, 102, 28041–28047, 1997.](#)

[Zhang, X. Y., Arimoto, R., Zhu, G. H., Chen, T., and Zhang, G. Y.: Concentration, size distribution and deposition of mineral aerosol over Chinese desert regions, *Tellus B*, 50, 317–330, 1998.](#)

[Zhang, X. Y., Gong, S. L., Shen, Z. X., Mei, F. M., Xi, X. X., Liu, L. C., Zhou, Z. J., Wang, D., Wang, Y. Q., and Cheng, Y.: Characterization of soil dust aerosol in China and its transport and distribution during 2001 ACE-Asia: I. Network observations, *J. Geophys. Res.*, 108, 4261, doi:10.1029/2002jd002632, 2003.](#)

zhang yan 8/2/15 7:52 PM

Deleted: Albani, S., N. M. Mahowald, A. T. Perry, R. A. Scanza, C. S. Zender, N. G. Heavens, V. Maggi, J. F. Kok, and B. L. Otto-Bliesner (2014), Improved dust representation in the Community Atmosphere Model, *J. Adv. Model. Earth Syst.*, 06, doi:10.1002/2013MS000279.

Main Tables 1- 5

Table 1a Generalized mineral compositions (%) applied in this study

Table 1b Elemental solubility as a percentage of the element contained in the minerals (%)

Table 2 Ten year averaged emission rates (Tg/yr) and percentages of elements over desert regions (%)

[Table 3 Comparison of modeled and observed fractions of chemical elements in TSP and tuning ratio based on 14-site measurements](#)

Table 4 Fractions (%) of elements in dust deposition into different ocean basins and ice sheets*

Table 5 Deposition of dust elements into different oceans and ice sheets*

Rachel Scanza 8/8/15 12:43 PM
Deleted: 4

zhang yan 8/2/15 8:37 PM
Formatted: Line spacing: multiple 1.15 li

zhang yan 8/2/15 8:35 PM
Deleted: 3

zhang yan 8/2/15 8:35 PM
Deleted: 4

Table1a Generalized mineral compositions (%) applied in this study

Mineral	Mg	P	Ca	Mn	Fe	Al	Si	K
Smectite	1.21	0.17	0.91	0.03	2.55	8.57	27.44	0.27
Illite	0.85	0.09	1.45	0.03	4.01	10.47	24.11	4.28
Hematite	0.09	0.18	0.12	0.07	57.50	2.67	2.11	0.07
Feldspar	0.15	0.09	3.84	0.01	0.34	10.96	25.24	5.08
Kaolinite	0.02	0.16	0.03	0.01	0.24	20.42	20.27	0.00
Calcite	0.00	0.00	40.00	0.00	0.00	0.00	0.00	0.00
Quartz	0.00	0.00	0.00	0.00	0.00	0.00	46.70	0.00
Gypsum	0.00	0.00	23.30	0.00	0.00	0.00	0.00	0.00

Table1b Elemental solubility as a percentage of the element contained in the minerals (%)

Mineral	Mg	P	Ca	Mn	Fe	Al	Si	K
Smectite	14.09	2.93	79.20	25.35	2.60	0.00	0.05	31.41
Illite	7.80	30.58	50.96	24.93	1.17	0.15	0.05	2.87
Hematite	0.00	0.00	0.00	3.39	0.01	0.00	0.00	0.00
Feldspar	5.17	0.00	4.46	4.71	3.01	0.12	0.02	4.53
Kaolinite	22.32	0.00	21.97	0.00	4.26	0.38	0.37	0.00
Calcite	0.00	0.00	7.00	0.00	0.00	0.00	0.00	0.00
Quartz	0.00	0.00	0.00	0.00	0.00	0.00	0.0003	0.00
Gypsum	0.00	0.00	0.56	0.00	0.00	0.00	0.00	0.00

*Fe content came from Journet et al. (2008), the other elements were from personal communication with E. Journet.

Rachel Scanza 8/8/15 12:39 PM
Deleted :

1
2
3
4
5

Table 2 Ten year averaged emission rates (Tg/yr) and percentages of elements over desert regions (%)

(For this table, annual mean emission of each element is divided by the annual mean emission of dust to obtain the %.)

Source Regions	Mg	P	Ca	Mn	Fe	K	Al	Si	Dust
WAsia	0.91	1.77E-01	12.73	3.53E-02	5.53	3.70	16.71	72.43	251.17
NCAasia	0.50	9.27E-02	6.05	1.80E-02	2.26	1.90	8.36	37.99	128.59
CAasia	0.13	2.54E-02	1.57	4.98E-03	0.70	0.55	2.35	9.77	33.82
SCAsia	0.05	1.07E-02	0.54	1.93E-03	0.29	0.22	1.04	4.07	13.91
EAsia	0.21	4.38E-02	1.62	8.16E-03	1.28	0.85	4.22	18.27	58.90
Asian Region	1.79	3.50E-01	22.52	6.84E-02	10.06	7.23	32.67	142.54	486.4
ESah	1.23	2.74E-01	11.98	4.83E-02	6.62	5.41	26.45	102.59	346.16
WSah	2.62	5.31E-01	30.67	1.01E-01	14.25	11.04	50.35	208.70	712.00
SNAf	0.02	1.17E-02	0.17	1.47E-03	0.37	0.12	1.25	4.33	13.98
SAf	0.01	3.10E-03	0.18	5.90E-04	0.11	0.06	0.31	1.34	4.46
Africa	3.89	8.20E-01	42.99	1.51E-01	21.34	16.63	78.36	316.96	1076.6
NWNAm	0.00002	4.70E-06	0.0001	8.00E-07	0.0002	0.0001	0.0005	0.0019	0.030
SWNAm	0.02	3.01E-03	0.16	6.00E-04	0.10	0.07	0.29	1.27	4.20
North America	0.02	3.02E-03	0.16	6.00E-04	0.10	0.07	0.29	1.27	4.2
SAm	0.0005	1.20E-04	0.01	2.00E-05	0.003	0.002	0.01	0.04	0.15
Palag	0.03	6.79E-03	0.27	1.32E-03	0.20	0.13	0.62	2.82	9.08
South America	0.03	6.91E-03	0.27	1.34E-03	0.21	0.13	0.63	2.86	9.2
WAsr	0.0005	1.30E-04	0.003	2.00E-05	0.003	0.002	0.01	0.05	0.16
EAsr	0.02	5.13E-03	0.20	9.10E-04	0.16	0.10	0.48	1.78	6.11
Australia region	0.02	5.26E-03	0.20	9.30E-04	0.17	0.10	0.49	1.83	6.3
Glbbl	5.75	1.18E+00	66.14	2.22E-01	31.87	24.15	112.44	465.46	1582.7
Global mean % element	0.36	0.07	4.18	0.01	2.01	1.53	7.10	29.41	/
Min. % element in 15 SR*	0.17	0.07	1.19	0.01	1.67	0.86	6.50	28.84	/
Max. % element in 15 SR*	0.39	0.08	5.07	0.02	2.68	1.63	8.96	31.38	/

6 *SR refer to source regions

7

janice 8/10/15 11:22 AM
Deleted: -

janice 8/10/15 11:04 AM
Deleted: -

10 [Table 3 Comparison of modeled and observed fractions of chemical elements in TSP, and tuning](#)
 11 [ratio based on 13-site measurements. \(For this table comparing the elemental ratios at the](#)
 12 [measurement sites, the % value at each time measured is averaged across time and space for this](#)
 13 [comparison.\)](#)

	Mg	P	Ca	Mn	Fe	K	Al
Corr. coeff. Of Averaged Fractions	0.14	-0.32	0.75	-0.51	0.29	-0.16	0.72
Median of Obs. (%)	1.45	0.09	5.42	0.070	3.10	1.79	5.26
Median of Mod.(%)	0.43	0.08	3.41	0.020	2.29	1.54	7.81
Obs./Mod. Median Ratio (tuned ratio)	3.4	1.1	1.6	3.5	1.4	1.2	0.7

janice 8/7/15 9:09 PM
Deleted: the concentrations

14
 15
 16 [Table 4 Fractions \(%\) of elements in dust deposition into different ocean basins and ice sheets*](#)

Ocean Basins/Glacier	Mg	P	Ca	Mn	Fe	K	Al	Si**
North Atlantic	1.43	0.10	5.36	0.06	3.05	1.89	5.96	28.32
South Atlantic	1.50	0.10	5.36	0.06	3.35	1.84	6.01	28.07
North Pacific	1.56	0.10	5.92	0.06	3.26	1.90	5.78	28.01
South Pacific	1.47	0.10	5.30	0.06	3.87	1.86	6.15	27.61
North Indian	1.38	0.08	7.90	0.05	3.13	1.81	4.95	28.29
South Indian	1.53	0.10	6.50	0.06	3.64	1.87	5.88	27.33
Southern Ocean	1.56	0.10	5.12	0.06	3.74	1.88	5.88	28.25
Arctic	1.60	0.10	6.23	0.06	3.31	1.96	5.76	27.76
Mediterranean	1.37	0.08	7.14	0.05	2.90	1.88	4.85	29.14
Antarctic ice sheets	1.50	0.10	4.90	0.06	3.54	1.82	5.55	29.17
Greenland ice sheets	1.50	0.09	7.49	0.06	2.82	1.89	5.24	28.00
Averaged	1.49	0.10	6.11	0.06	3.33	1.87	5.64	28.18

Cornell University 8/6/15 10:23 AM
Formatted: Left

zhang yan 8/2/15 8:35 PM
Deleted: 3

17 *After timing tuned ratios (Table 3) except for Si

zhang yan 8/2/15 8:38 PM
Deleted: B4

18 ** Not tuning

19 (For this table, annual mean deposition of each element is divided by the annual mean deposition of
 20 dust to obtain the %.)

21

22

janice 8/10/15 11:04 AM
Deleted:

Table 5. Deposition of dust elements into different oceans and ice sheets *

Ocean / ice sheet	Mg (Tg/yr)		P (Gg/yr)		Ca (Tg/yr)		Mn (Gg/yr)		Fe (Tg/yr)		K (Tg/yr)							
	Sol-1	Sol-2	Sol-1	Sol-2	Sol-1	Sol-2	Sol-1	Sol-2	Sol-1	Sol-2	Sol-1	Sol-2						
North Atlantic	1.50	0.16	0.14	103.12	8.81	4.10	5.64	0.68	1.81	58.90	12.08	3.87	3.20	0.036	0.033	1.99	0.008	0.136
South Atlantic	0.13	0.01	0.02	8.84	0.79	0.38	0.47	0.06	0.17	5.17	1.07	0.34	0.30	0.003	0.003	0.16	0.007	0.014
North Pacific	0.28	0.03	0.03	17.47	1.66	0.65	1.06	0.13	0.33	10.58	2.25	0.58	0.58	0.007	0.006	0.34	0.014	0.025
South Pacific	0.01	0.001	0.001	0.86	0.07	0.04	0.04	0.006	0.01	0.50	0.10	0.03	0.03	0.0003	0.000	0.02	0.0007	0.001
North Indian	0.56	0.06	0.06	34.38	3.54	1.52	3.23	0.29	0.63	21.86	4.62	1.35	1.28	0.013	0.013	0.74	0.03	0.049
South Indian	0.05	0.005	0.005	3.03	0.30	0.20	0.20	0.02	0.05	1.85	0.39	0.16	0.11	0.001	0.001	0.06	0.002	0.004
Southern Ocean	0.002	0.0003	0.0003	0.15	0.01	0.01	0.01	0.001	0.003	0.09	0.02	0.01	0.01	0.0001	0.0001	0.00	0.0001	0.0002
Arctic	0.02	0.002	0.0020	1.34	0.13	0.05	0.09	0.01	0.02	0.83	0.18	0.04	0.05	0.0005	0.0004	0.03	0.001	0.002
Mediterranean	0.18	0.02	0.02	10.66	1.07	0.36	0.92	0.09	0.22	6.76	1.42	0.36	0.37	0.004	0.004	0.24	0.011	0.017
Antarctic ice sheets	0.001	0.0001	0.0001	0.08	0.007	0.003	0.00	0.001	0.002	0.05	0.01	0.003	0.00	0.00003	0.00003	0.00	0.0001	0.0001
Greenland ice sheets	0.09	0.01	0.01	5.39	0.49	0.21	0.44	0.04	0.10	3.30	0.71	0.19	0.17	0.002	0.002	0.11	0.005	0.007
Total	2.83	0.30	0.28	185.32	16.89	7.52	12.11	1.32	3.35	109.89	22.84	6.95	6.10	0.068	0.06	3.69	0.153	0.25

*Here the soluble element deposition using Sol-1 has been tuned by timing tuned ratios (Table 3); Sol-1 refer to mineral method after tuning, Sol-2 refer to Stillanpa method described in the methods section (2).

Janice 8/10/15 11:03 AM
 Formatted: Left: 2.5 cm, Right: 2.5 cm,
 Top: 3.17 cm, Bottom: 3.17 cm, Width:
 29.7 cm, Height: 21 cm

Zhang Yan 8/21/15 8:38 PM
 Deleted: 4

Main Figures 1- 15

Fig.1. Observational sites (S1-Hetian, China; S2-Tazhong, China; S3-Yu Lin, China; S4-Duolun, China; S5-Shengsi, China; S6-Hanoi, Vietnam; S7-Marnila, Philippines; S8- Balad, Iraq; S9-Balad, Iraq; S10-Taji, Iraq; S11-Eilat; S12-Cape Verde Atmospheric Observatory (CVAO); S13-Muswellbrook, Australia; S14-Richmond, Australia; S15-Tamanrasset, Algeria; S16-Banizoumbou, Niger; S17-Douz, Tunisia) **and dust-producing regions** (WAsia: West Asia; NC-As: North Central Asia; CAsia: Central Asia; SC-As: South Central Asia; EAsia:East Asia; WN-Af:North West Africa; EN-Af: North East Africa; S-NAf: Southern North Africa; SAf: Southern Africa; MWNA: Middle North West America; SWNA: Southern North West America; SAm1: Northern South America; SAm2: Southern South America; WAus: West Australia; EAus: East Australia)

Fig.2 Global elemental distributions (in mass percentage) in a1: Clay Mg, a2: Clay P, a3: Clay Ca, a4: Clay Mn, a5: Clay Fe, a6: Clay K, a7:, Clay Al, a8: Clay Si; b1: Silt Mg, b2: Silt P, b3: Silt Ca, b4: Silt Mn, b5: Silt Fe, b6: Silt K, b7: Silt Al, b8: Silt Si.

Fig.3 Global mean elemental percentages in (a) four-bin dust emission and (b) clay and silt fractions of soils (Bin1-4 refer to particle range listed in Table S2, clay refer to < 2um, silt refer to > 2um)

Fig.4 Percentages of elements in dust concentration (mass %): a. Mg, b. P, c. Ca, d. Mn, e. Fe, f. K, g. Al, h. Si. Elemental % shown here are calculated using the annual mean element concentration divided by the annual mean dust concentration.

Fig.5 Ratio of mass fractions of elements in dust deposition to that in atmospheric dust: a. Mg, b. P, c. Ca, d. Mn, e. Fe, f. K, g. Al, h. Si. Elemental ratios shown here are calculated using the annual mean element deposition divided by the annual mean dust deposition.

Fig.6 Ten-year monthly variability in mean of elemental percentages in atmospheric dust (mass %): a. Mg, b. P, c. Ca, d. Mn, e. Fe, f. K, g. Al, h. Si. Elemental monthly mean % are calculated using the monthly mean emission of each element divided by the monthly mean emission of dust.

Fig.7 Ten-year monthly variability in mean of elemental percentages in dust deposition (mass %):a. Mg, b. P, c. Ca, d. Mn, e. Fe, f. K, g. Al, h. Si. Elemental monthly mean % are calculated using the monthly mean emission of each element divided by the monthly mean emission of dust.

Fig.8 Ca/Al in Soil and ten year averaged Ca/Al ratio in dust emission, concentration and deposition. Top two (a,b) refer to ratio in clay and silt desert soil, middle one (c) refer to ratio in dust emission, and bottom two (d,e) refer to

janice 8/10/15 11:04 AM

Deleted: Page Break

janice 8/10/15 11:04 AM

Formatted: Space After: 0 pt, Line spacing: single

63 [ratio in dust concentration and deposition. Elemental annual mean % are calculated using the annual mean](#)
64 [emission of each element divided by the annual mean emission of dust.](#)

65 [Fig.9 Ten year averaged Ca/Al ratio in \(a\) dust emission of source regions and \(b\) dust deposition into various ocean](#)
66 [basins and glaciers. Elemental ratios are calculated using the annual mean emission of Ca divided by the annual](#)
67 [mean emission of Al.](#)

68 [Fig.10 Comparison of observed and modeled mean fractions of elements at each site for \(a\) total](#)
69 [suspended particulates \(TSP\) and \(b\) PM_{2.5}. \(1-Hetian, China; 2-Tazhong, China; 3-Yu Lin, China;](#)
70 [4-Duolun, China; 5-Shengsi, China; 6-Hanoi, Vietnam; 7-Marnila, Philippines; 8-Balad, Iraq;](#)
71 [9-Baghdad, Iraq; 10-Taji,Iraq; 11-Eilat; 12-Cape Verde Island; 13-Muswellbrook, Australia;](#)
72 [14-Richmond, Australia, 15-Tamanrasset, Algeria; 16-Banizoumbou, Niger; 17-Douz, Tunisia\). Here](#)
73 [we calculate the elemental fractions and average the fractions temporally for each site and compare to](#)
74 [observations.](#)

75

76 [Fig.11 Mean and quartile modeled and observational fractions of elements in \(a\) TSP \(b\) PM_{2.5} for all](#)
77 [sites together, the box line presents 25%, 50% and 75%, individually. Here we calculate the elemental](#)
78 [fractions and average the fractions temporally for each site and compare to observations.](#)

79

80 [Fig.12 \(a\) Observational and \(b\) modeled dust deposition \(g/m³/year\). The scale is the same for both](#)
81 [panels. \(c\) A scatterplot shows the comparison between the model and observations. The correlation](#)
82 [coefficient between observations and model results reach 0.86.](#)

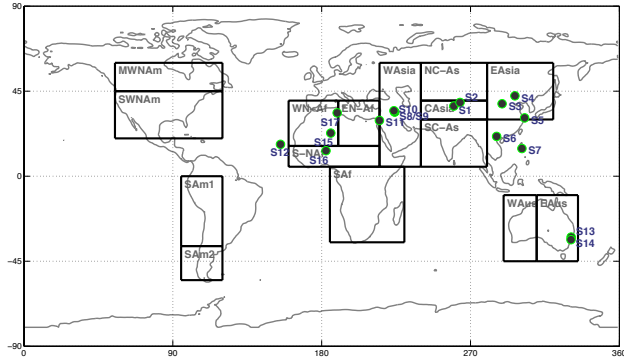
83 [Fig.13 Percentages of elements in dust deposition \(%\) after tuning. It is tuned based on original](#)
84 [percentages of elements in dust deposition in Fig. S1 by ~~using~~ tuning Obs./Mod. ratios listed in Table 3. Si](#)
85 [did not change because there are not enough observational data available](#)

86 [Fig. 14 Fractional solubility of elements \(soluble element / total element\) in dust deposition \(%\):a. Mg, b.](#)
87 [P, c. Ca, d. Mn, e. Fe, f. K, g. Al, h. Si](#)

88 [Fig. 15 Percentages of soluble elements in total dust deposition using\(a\) Sol-1 & \(b\) Sol-2 \(%\), Sol-1](#)
89 [refer to mineral method after tuning, Sol-2 refer to Sillanpaa method described in the methods section](#)
90 [\(2\).](#)

janice 8/10/15 11:03 AM

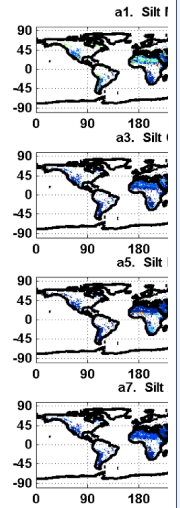
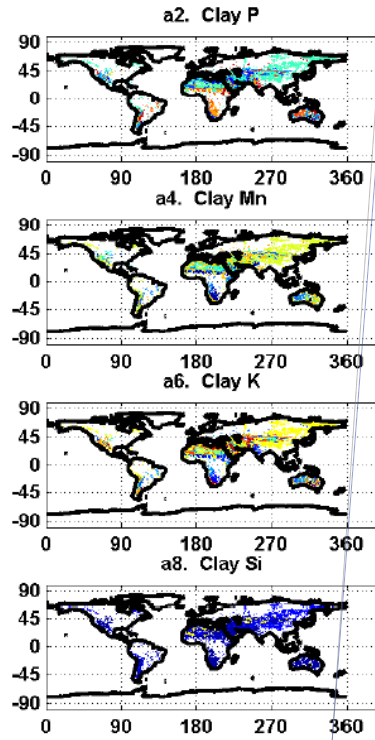
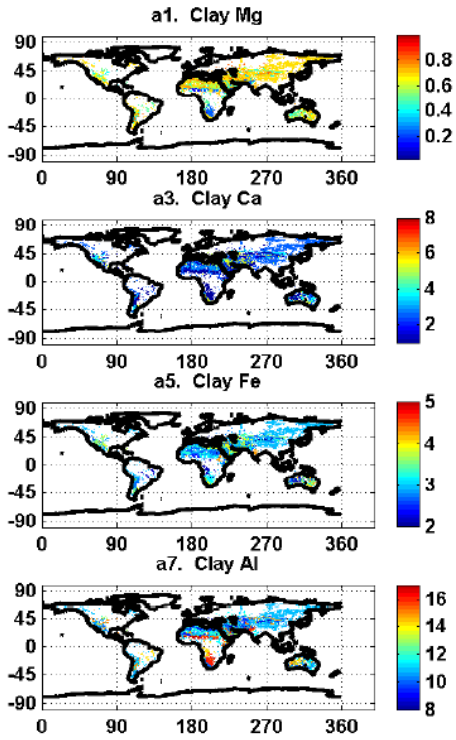
Deleted: ratio



92

93 **Fig.1. Observational sites** (S1-Hetian, China; S2-Tazhong, China; S3-Yu Lin, China; S4-Duolun,
 94 China; S5-Shengsi, China; S6-Hanoi, Vietnam; S7-Marnila, Philippines; S8- Balad, Iraq; S9-Balad,
 95 Iraq; S10-Taji, Iraq; S11-Eilat; S12-Cape Verde Atmospheric Observatory (CVAO);
 96 S13-Muswellbrook, Australia; S14-Richmond, Australia; S15-Tamanrasset, Algeria;
 97 S16-Banizoumbou, Niger; S17-Douz, Tunisia) **and dust-producing regions** (WAsia: West Asia;
 98 NC-As: North Central Asia; CAsia: Central Asia; SC-As: South Central Asia; EAsia:East Asia;
 99 WN-Af:North West Africa; EN-Af: North East Africa; S-NAf: Southern North Africa; SAF: Southern
 100 Africa; MWNAf: Middle North West America; SWNAf: Southern North West America; SAm1:
 101 Northern South America; SAm2: Southern South America; WAus: West Australia; EAus: East
 102 Australia)

103



104

105

(a) in soil_clay

Unknown

Formatted: Font:(Default) Times New Roman, 10 pt

janice 8/10/15 4:46 PM

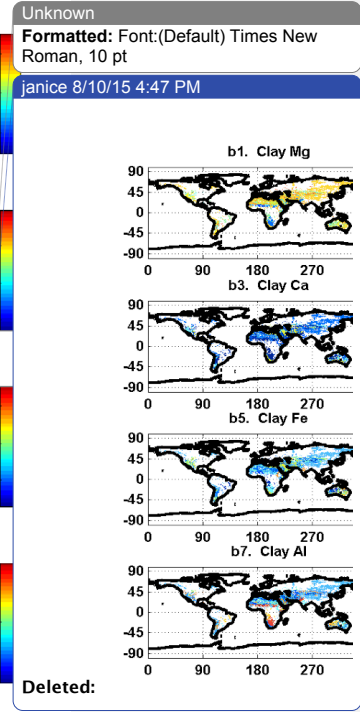
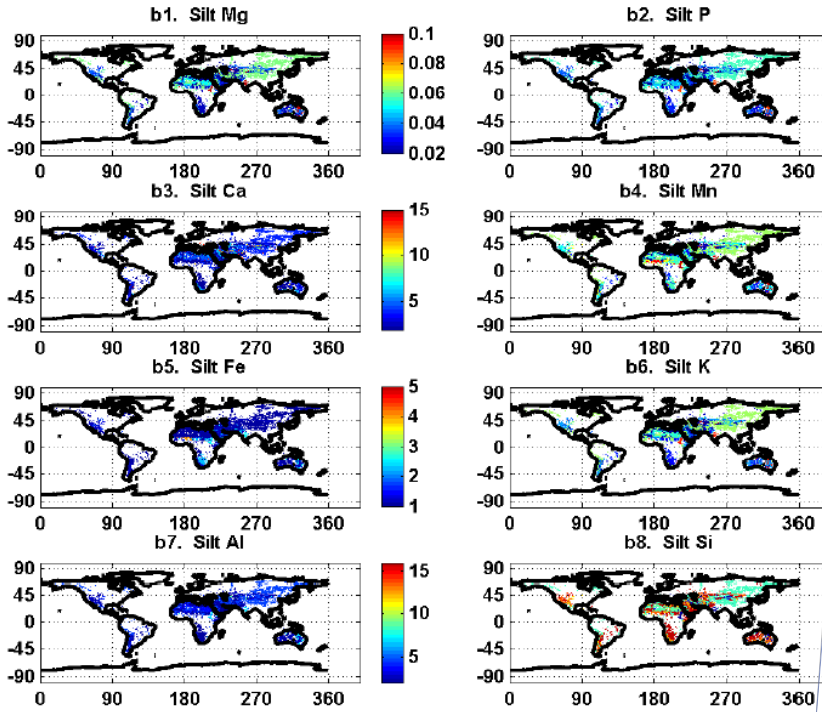
Deleted:

janice 8/10/15 4:46 PM

Deleted: silt

zhang yan 8/8/15 1:02 AM

Formatted: Centered



108

109

110

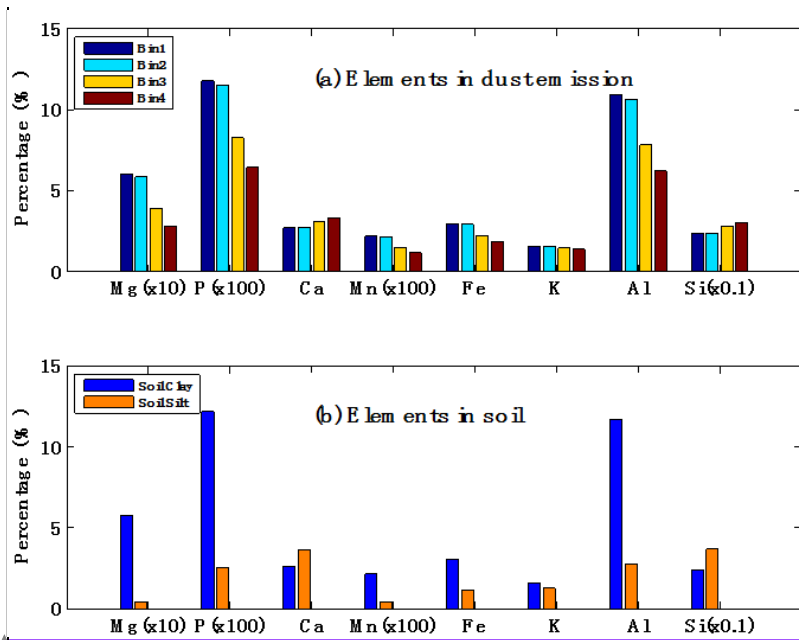
111

112

(b) in soil silt

Fig.2 Global elemental distributions (in mass percentage) in (a) soil clay, a1: Clay Mg, a2: Clay P, a3: Clay Ca, a4: Clay Mn, a5: Clay Fe, a6: Clay K, a7: Clay Al, a8: Clay Si; (b) soil silt, b1: Silt Mg, b2: Silt P, b3: Silt Ca, b4: Silt Mn, b5: Silt Fe, b6: Silt K, b7: Silt Al, b8: Silt Si.

janice 8/10/15 4:46 PM
Deleted: clay
zhang yan 8/8/15 1:01 AM
Formatted: Centered



Unknown
 Formatted: Font:(Default) Times New Roman, 9 pt
 ras486 8/9/15 3:26 PM
 Formatted: Indent: Left: -0.98 ch, Hanging: 1 ch

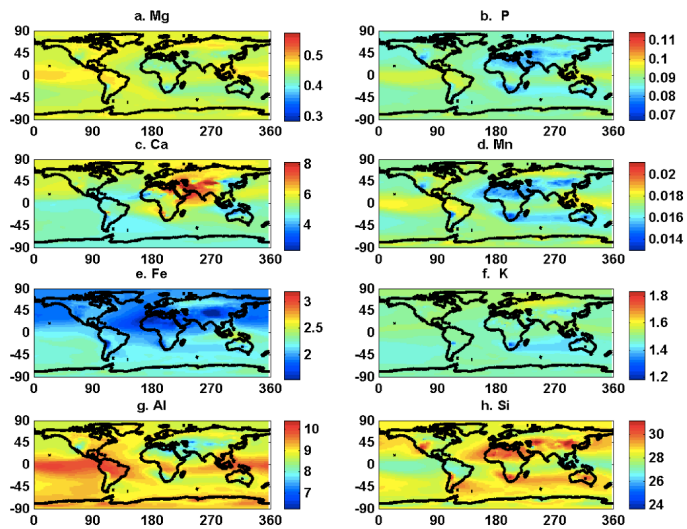
115

116 [Fig.3 Global mean elemental percentages in \(a\) four-bin dust emission and \(b\) clay and silt fractions of soils \(Bin1-4](#)

117 [refer to particle range listed in Table S2, clay refer to < 2 \$\mu\$ m, silt refer to > 2 \$\mu\$ m\)](#)

118

119



120

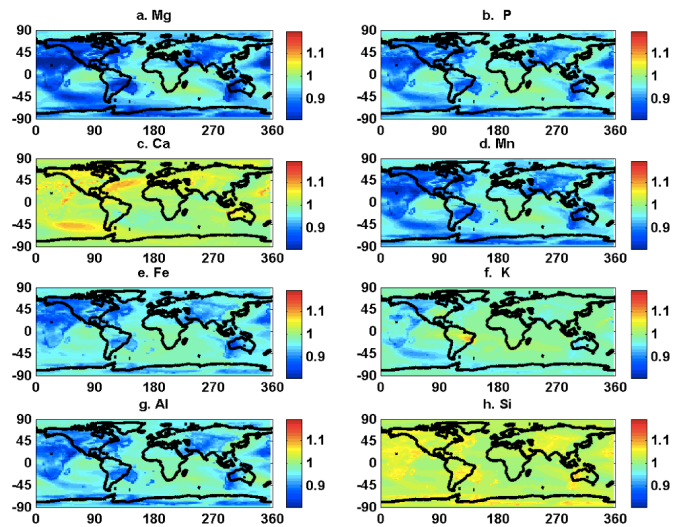
121 [Fig.4 Percentages of elements in dust concentration \(mass %\) : a. Mg, b. P, c. Ca, d. Mn, e. Fe, f. K, g. Al, h. Si.](#)

122 [Elemental % shown here are calculated using the annual mean element concentration divided by the annual mean](#)

123 [dust concentration.](#)

124

Unknown
Formatted: Font:(Default) Times New Roman, 9 pt
ras486 8/9/15 3:26 PM
Formatted: Indent: Left: -0.98 ch, Hanging: 1 ch



126

127 [Fig.5 Ratio of mass fractions of elements in dust deposition to that in atmospheric dust : a. Mg, b. P, c. Ca, d. Mn, e.](#)
 128 [Fe, f. K, g. Al, h. Si. Elemental ratios shown here are calculated using the annual mean element deposition divided](#)
 129 [by the annual mean dust deposition.](#)

Unknown

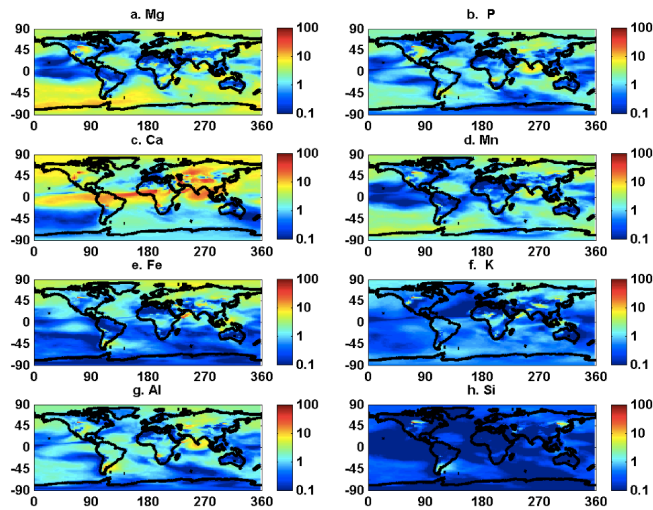
Formatted: Font:(Default) Times New Roman, 9 pt

ras486 8/9/15 3:26 PM

Formatted: Indent: Left: -0.98 ch, Hanging: 1 ch

Unknown
Formatted: Font:(Default) Times New Roman, 9 pt

ras486 8/9/15 3:26 PM
Formatted: Indent: Left: -0.98 ch, Hanging: 1 ch



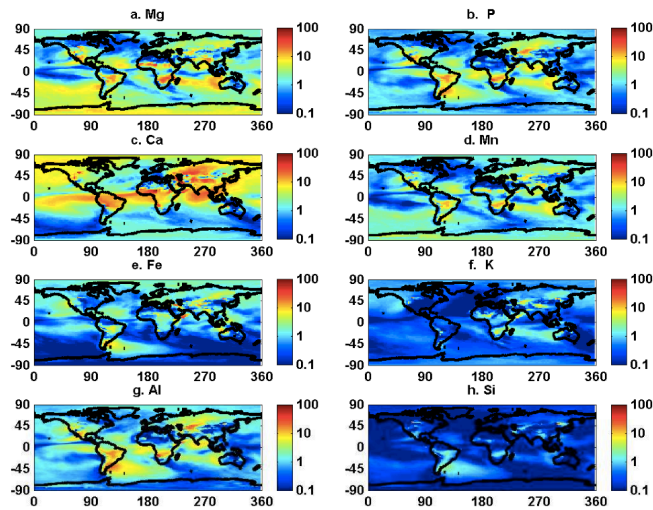
130

131 [Fig.6 Ten-year monthly variability in mean of elemental percentages in atmospheric dust \(mass % \) : a. Mg, b. P, c.](#)
132 [Ca, d. Mn, e. Fe, f. K, g. Al, h. Si. Elemental monthly mean % are calculated using the monthly mean emission of](#)
133 [each element divided by the monthly mean emission of dust.](#)

134

Unknown
Formatted: Font:(Default) Times New Roman, 9 pt

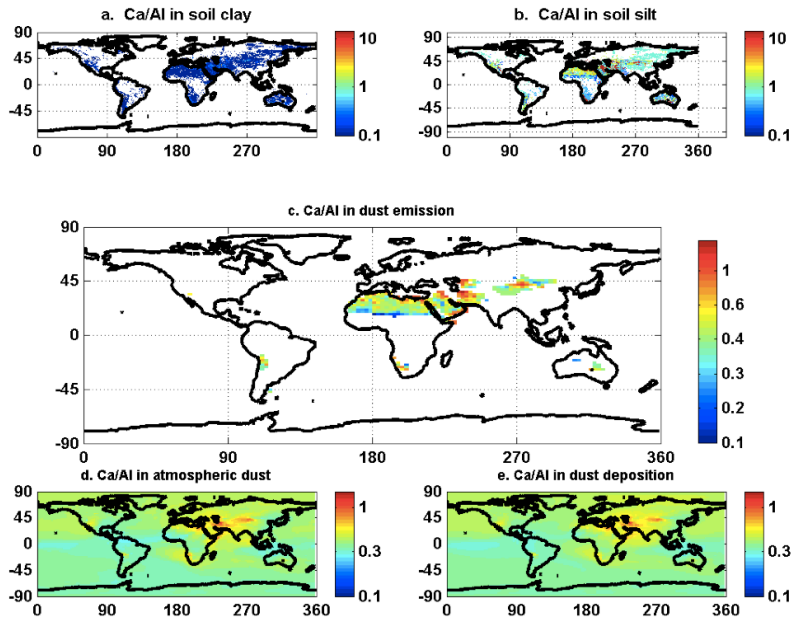
ras486 8/9/15 3:26 PM
Formatted: Indent: Left: -0.98 ch, Hanging: 1 ch



135

136 [Fig.7 Ten-year monthly variability in mean of elemental percentages in dust deposition \(mass %\):a. Mg, b. P, c. Ca,](#)
137 [d. Mn, e. Fe, f. K, g. Al, h. Si. Elemental monthly mean % are calculated using the monthly mean emission of each](#)
138 [element divided by the monthly mean emission of dust.](#)

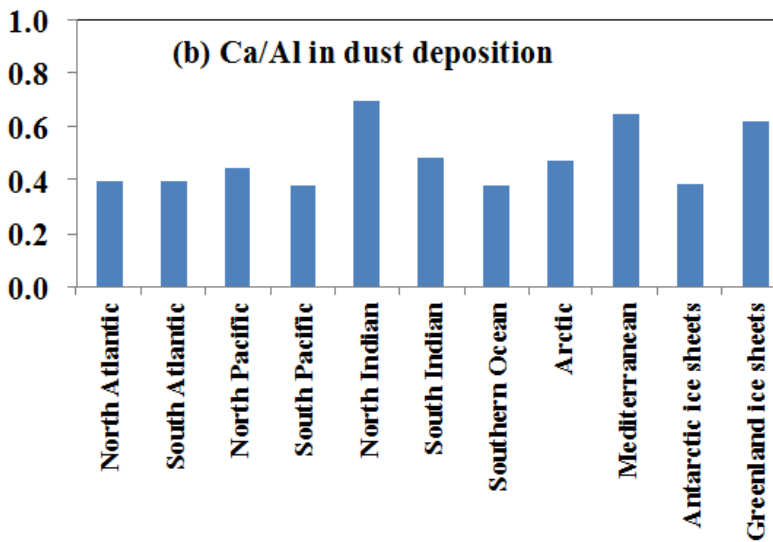
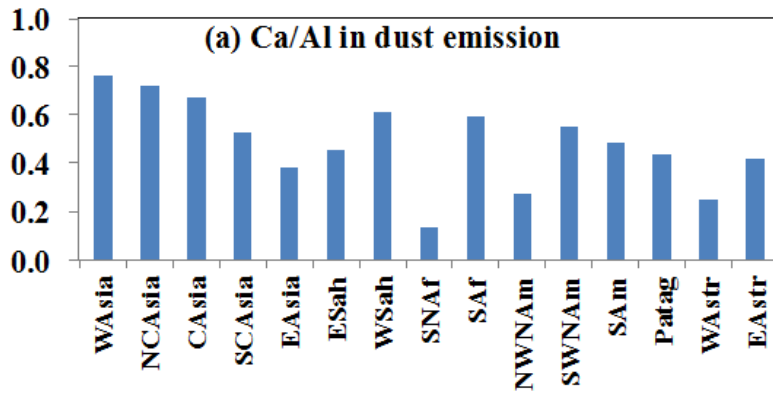
139



Unknown
 Formatted: Font:(Default) Times New Roman, 9 pt
 ras486 8/9/15 3:26 PM
 Formatted: Indent: Left: -0.98 ch, Hanging: 1 ch

140
 141
 142
 143
 144
 145
 146

Fig.8 Ca/Al in Soil and ten year averaged Ca/Al ratio in dust emission, concentration and deposition. Top two (a,b) refer to ratio in clay and silt desert soil, middle one (c) refer to ratio in dust emission, and bottom two (d,e) refer to ratio in dust concentration and deposition. Elemental annual mean % are calculated using the annual mean emission of each element divided by the annual mean emission of dust.



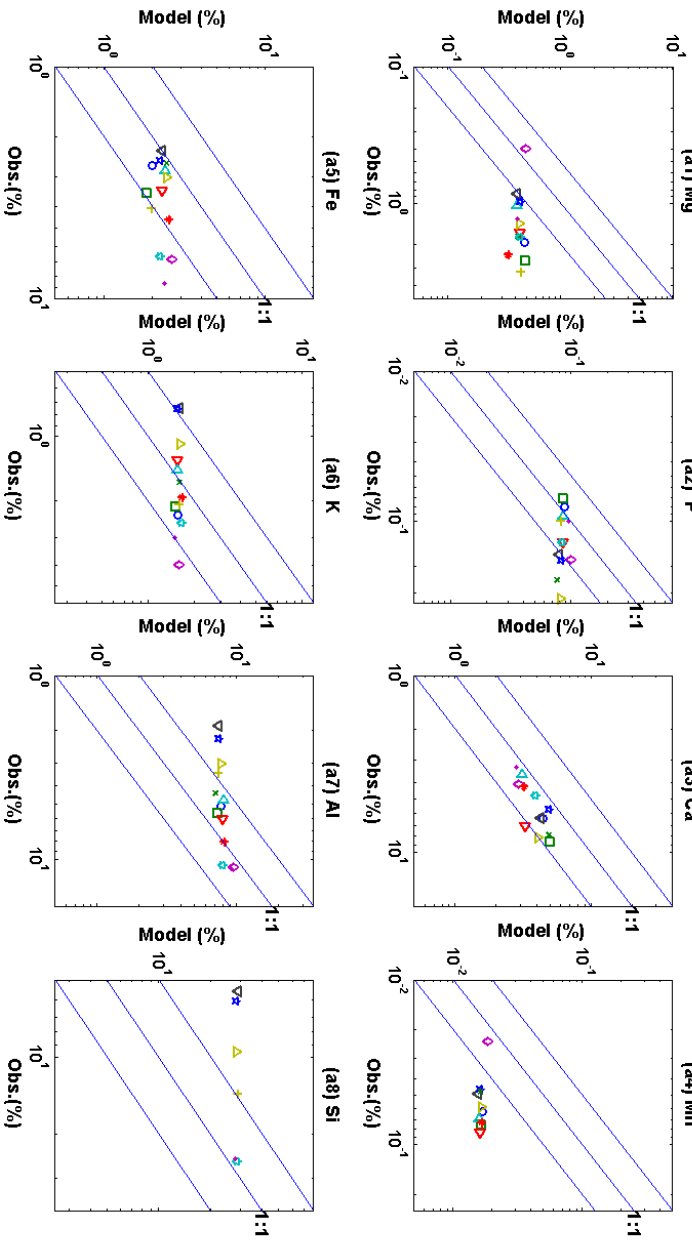
147

148 Fig.9 Ten year averaged Ca/Al ratio in (a) dust emission of source regions and (b) dust deposition into various ocean
 149 basins and glaciers. Elemental ratios are calculated using the annual mean emission of Ca divided by the annual
 150 mean emission of Al.

Unknown
 Formatted: Font:(Default) Times New Roman, 9 pt
 ras486 8/9/15 3:26 PM
 Formatted: Indent: Left: -0.98 ch, Hanging: 1 ch

Sites:

- 1
- 2
- 3
- 4
- 5
- 8
- 9
- 10
- 11
- 12
- 15
- 16
- 17



(a) TSP

151
152

42

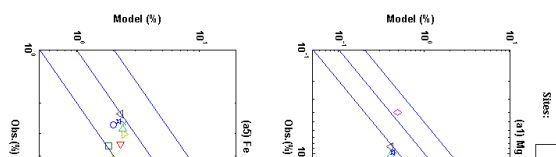
Unknown

Formatted: Font:(Default) Times New Roman, 9 pt

Zhang yan 8/14/15 9:52 PM

Formatted: Indent: Left: -0.98 ch, Hanging: 1 ch

Janice 8/10/15 3:30 PM



Deleted:

Rachel Scanza 8/8/15 6:57 PM

Formatted: Centered

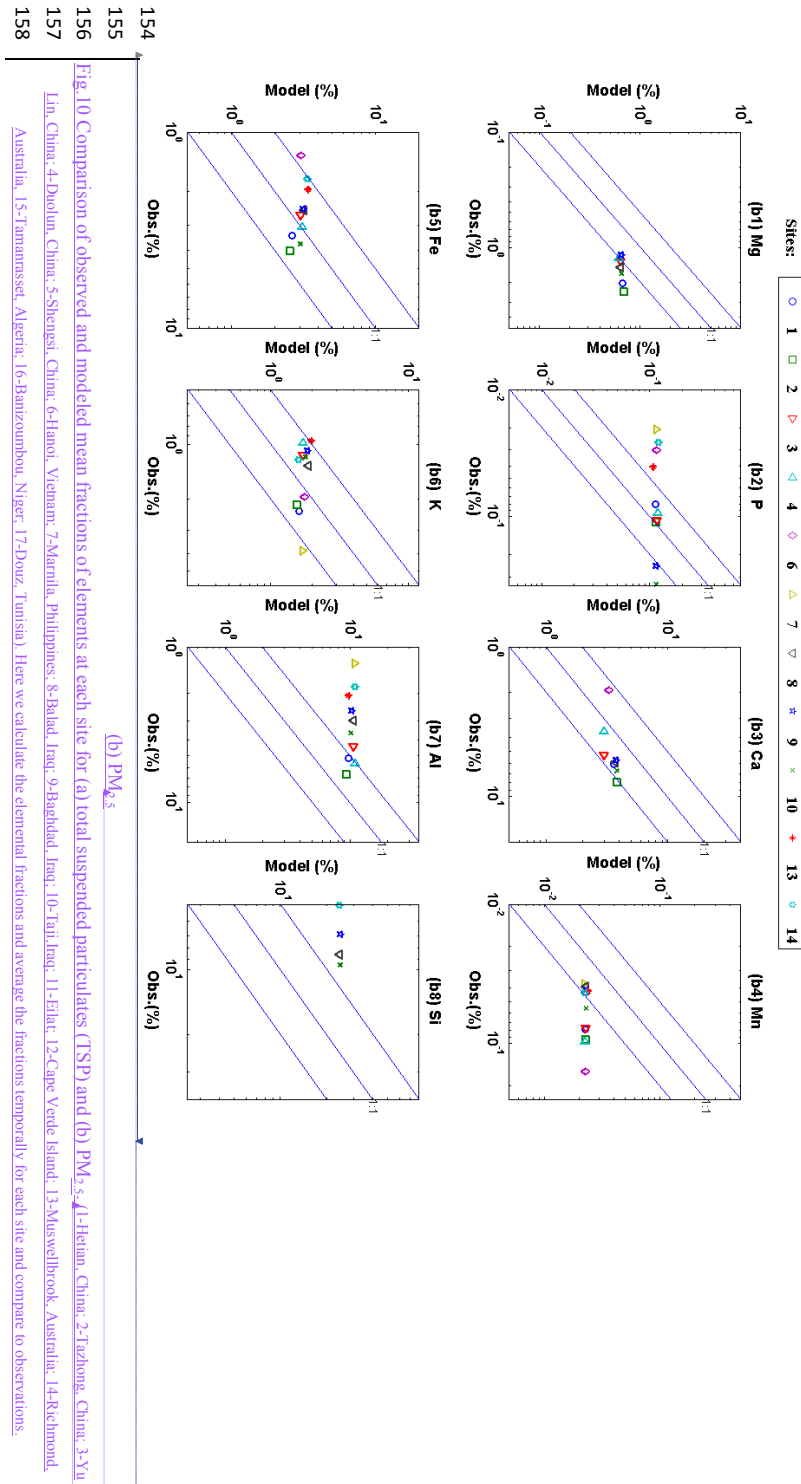


Fig. 10 Comparison of observed and modeled mean fractions of elements at each site for (a) total suspended particulates (TSP) and (b) $PM_{2.5}$. 1-Hetian, China; 2-Tazhong, China; 3-Yu Lin, China; 4-Duolin, China; 5-Shengsi, China; 6-Hanoi, Vietnam; 7-Mariña, Philippines; 8-Bahad, Iraq; 9-Baqubah, Iraq; 10-Taji, Iraq; 11-Eilat, 12-Cape Verde Island; 13-Muswellbrook, Australia; 14-Richmond, Australia; 15-Tamanrasset, Algeria; 16-Banzoumbou, Niger; 17-Douz, Tunisia. Here we calculate the elemental fractions and average the fractions temporally for each site and compare to observations.

43

Unknown

Formatted: Font:(Default)
TimesNewRomanPSMT, 10 pt

Zhang yan 8/11/15 9:52 PM

Formatted: Indent: Left: -0.98 ch,
Hanging: 1 ch

Janice 8/10/15 3:30 PM

Deleted:

Zhang yan 8/11/15 9:54 PM

Formatted: Centered

Zhang yan 8/8/15 12:54 AM

Formatted: Subscript

Zhang yan 8/11/15 10:01 PM

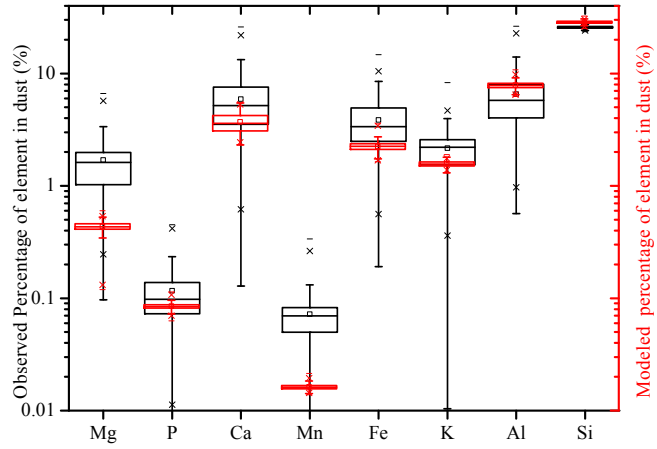
Formatted: Font:8 pt

Slices: |

(b1) Mg

(b5) Fe

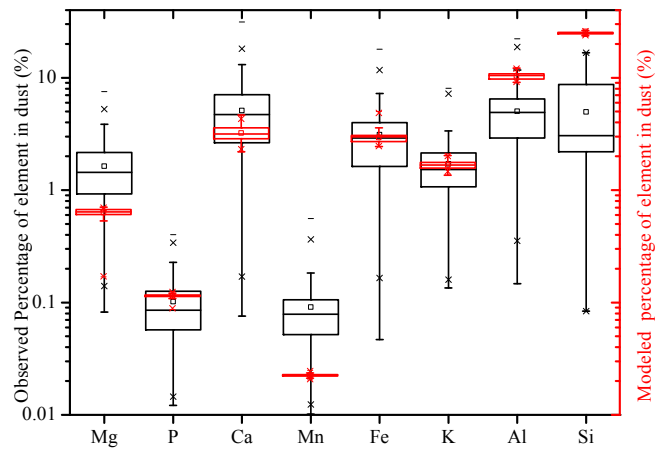
161



162

163

(a) TSP



164

165

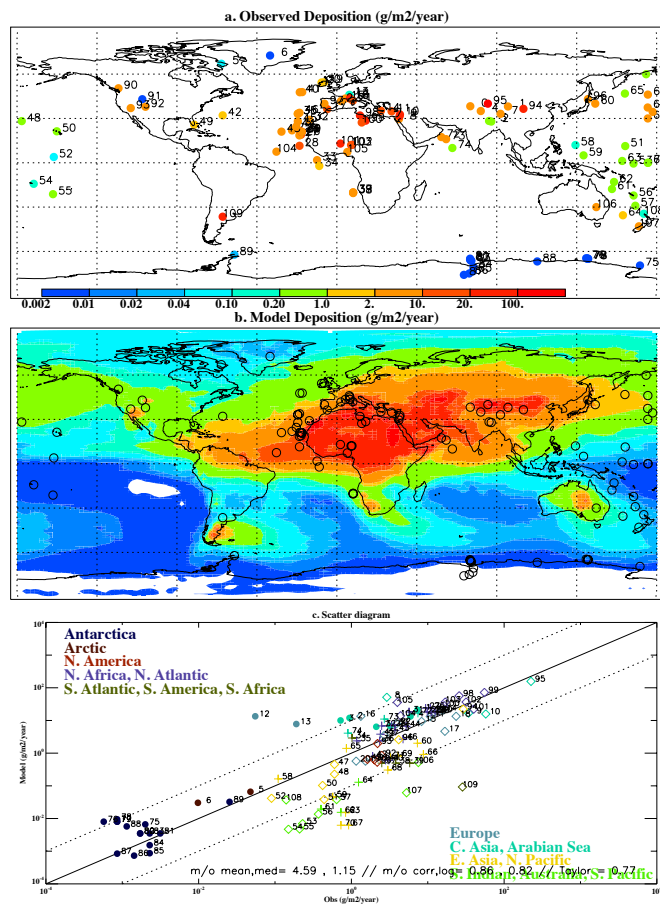
(b) PM_{2.5}

166 Fig.11 Mean and quartile modeled and observational fractions of elements in (a) TSP (b) PM_{2.5} for all
167 sites together, the box line presents 25%, 50% and 75%, individually. Here we calculate the elemental
168 fractions and average the fractions temporally for each site and compare to observations.

zhang y
Formatt
Unknow
Formatt
Roman,
ras486.8
Formatt
Hanging

zhang y
Formatt
Unknow
Formatt
Roman,

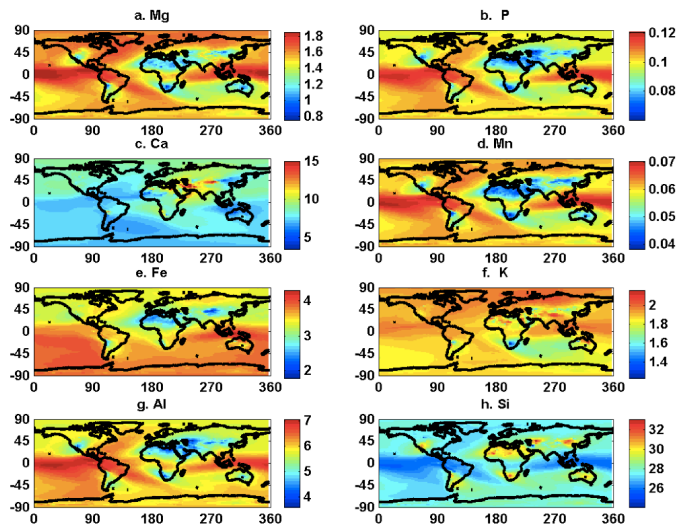
Rachel S
Formatt
zhang y
Formatt



Unknown
 Formatted: Font:(Default) Times New Roman, 10 pt
 ras486 8/9/15 3:26 PM
 Formatted: Indent: Left: -0.98 ch, Hanging: 1 ch

169

170 Fig.12 (a) Observational and (b) modeled dust deposition ($\text{g}/\text{m}^2/\text{year}$). The scale is the same for both
 171 panels. (c) A scatterplot shows the comparison between the model and observations. The correlation
 172 coefficient between observations and model results reach 0.86.

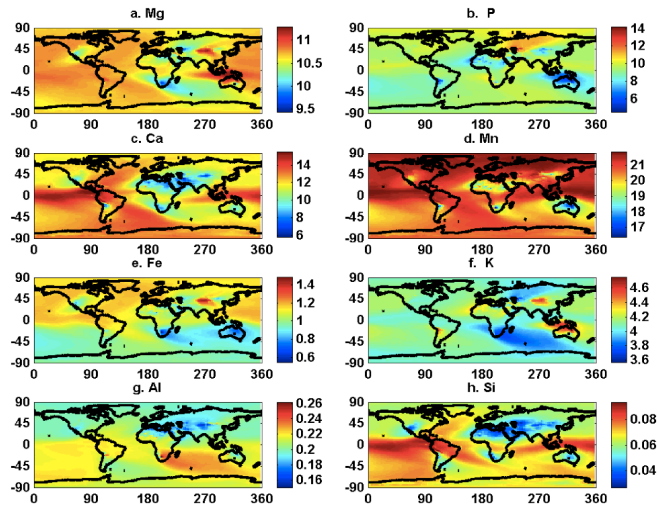


173

174 [Fig.13 Percentages of elements in dust deposition \(%\) after tuning. It is tuned based on original](#)
 175 [percentages of elements in dust deposition in Fig. S1 by fixing Obs./Mod. ratios listed in Table 3. Si](#)
 176 [did not change because there are not enough observational data available](#)

Unknown
 Formatted: Font:10 pt, Bold
 zhang yan 8/11/15 9:48 PM
 Formatted: Indent: Left: -0.98 ch,
 Hanging: 1 ch

janice 8/10/15 11:02 AM
 Deleted: ratio



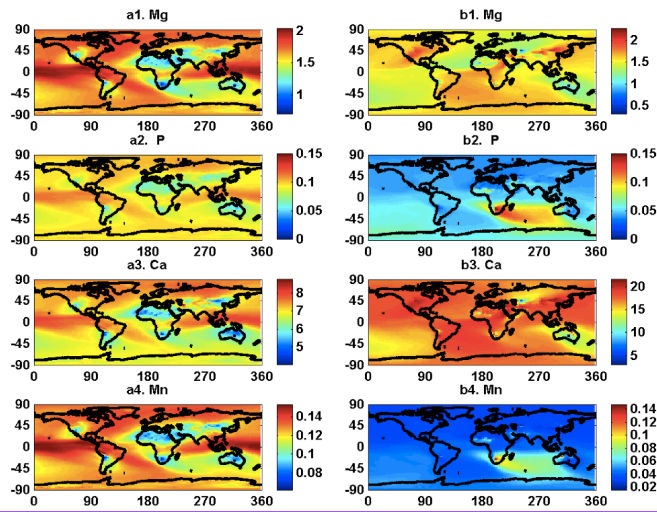
178

179 [Fig. 14 Fractional solubility of elements \(soluble element / total element\) in dust deposition \(%\)](#):a. Mg, b.
 180 [P, c. Ca, d. Mn, e. Fe, f. K, g. Al, h. Si](#)

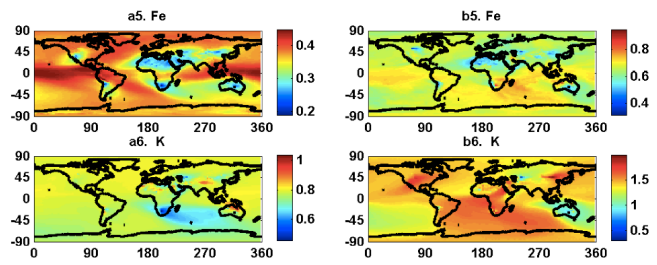
181

Unknown
 Formatted: Font:(Default) Times New Roman, 10 pt
 ras486 8/9/15 3:26 PM
 Formatted: Indent: Left: -0.98 ch, Hanging: 1 ch

182



183



184

185 [Fig. 15 Percentages of soluble elements in total dust deposition using \(a\) Sol-1 & \(b\) Sol-2 \(%\)](#). Sol-1
 186 [refer to mineral method after tuning](#), Sol-2 refer to [Sillanpaa method](#) described in the methods section
 187 [\(2\)](#).

188

Unknown
 Formatted: Font:(Default) Times New Roman, 10 pt
 ras486 8/9/15 3:26 PM
 Formatted: Indent: Left: -0.98 ch, Hanging: 1 ch

Unknown
 Formatted: Font:(Default) Times New Roman, 10 pt

zhang yan 8/2/15 8:38 PM
 Deleted: *After timing tuned ratio (Table B4) .